# Supraglacial lake evolution on the Greenland Ice Sheet

**Humphrey John Waddington**

St Catharine's College, Cambridge

12th June 2009

Scott Polar Research Institute

University of Cambridge

Lensfield Road

Cambridge CB2 1ER

England

**This dissertation is submitted for the degree of Master of Philosophy**

**This dissertation is the result of my own work, includes nothing that is the outcome of work done in collaboration with any other researchers except where specifically indicated in the text, and is not more than 20,000 words in length.**

*HJW, 12th June 2009*

**Acknowledgements**

The author would like to thank Dr Ian Willis for the motivation in choosing this topic of research, Dr Neil Arnold for his hard work in troubleshooting the problems arising from the numerical model code, Andreas Ahlstrøm for the provision of a DEM and delimited dataset, and Toby Benham for his tireless support and encouragement in using ArcView GIS and ERDAS Imagine software.

**Abstract.** Supraglacial lakes form annually on the surface of the Greenland Ice Sheet around Paakitsoq, north of the Jakobshavn Isbrae outlet glacier. The lakes are ephemeral, drain through moulins or crevasses at their bed throughout the melt season, and deliver large volumes of water to the subglacial hydrological system. Such inputs of water can cause spatially and temporally constrained speed-up events affecting the normally slow, marginally-terminating inland ice flow regimes. This dynamic response of the Greenland Ice Sheet to increased basal lubrication is likely to be influenced under global warming scenarios as more meltwater will be produced with increased temperatures. An understanding of the evolution of supraglacial lakes is helpful to understanding the volumes of water delivered to the subglacial hydrological system, and the present study focusing on Paakitsoq investigates lake volume evolution as observed in satellite imagery collected through the melt season in 2008, and through the use of a numerical model to predict lake inputs. The surface energy balance model used is a more advanced numerical model than has been used in previous study and model results are mixed. Conclusions are drawn from model and observed results, and suggest that with further investigation and manipulation, the model may provide accurate results that represent true melt water volumes, and the patterns of observed supraglacial lake evolution on the surface of the Greenland Ice Sheet. It is suggested that the present and future studies on surface lake evolution on the ice sheet would benefit from the collection of data from the Paakitsoq ice surface and from a higher resolution digital elevation model.

# Table of contents

# List of figures and tables

**Figure 9:** Elevation profile of the large lake shown in figure 4, derived from flightline traverse over the lake as shown in figure 2. Lake extents are given for 7th July 2001 and 24th June 2008 as shown in the lake margin positions from the respective LandSat images collected for these dates.

**Figure 10:** Surface elevation of the ice sheet and surrounding land-margin at Paakitsoq (contour elevations are meters above sea level; DEM extent is 80.5km by 67km). Ridges over the non-glaciated part of the study area (see figure 5) resulted from data manipulation during DEM kriging and interpolation.

**Figure 11:** (coloured) sinks in the DEM surface as visualized using the static supraglacial hydrological routing routine in ArcView 3.3 overlaid onto a collected (11th August 2008) greyscale LandSat image of the study area.

**Figure 12:** Supraglacial flow accumulation network as identified by the surface flow routing analysis in ArcView 3.3. Accumulation pathways are shown in green, with lighter colours indicating fewer upstream feeder cells than darker colours. Sinks are also identified in the image (shown as orange rectangles) and it is clear that in the central Paakitsoq region, surface drainage channels feed these sinks, and these individual channels (and surface lakes formed in the sinks) are often identifiable in the 2008 LandSat images. The three circled sinks and accumulation flow pathways leading into the sinks are discussed further in the text below.

**Figure 13:** Detail of three sinks and accumulation pathways (circled) that are identified as being lakes with surface channels in the June 2008 satellite image. The top image shows modelled surface drainage routes, while the bottom image shows the sinks as lakes with filled or relict channels feeding them that correspond well to the modelled drainage routes. These sinks exhibit lakes within c.400m of their modelled position in the June and July 2008 LandSat images, although the lakes have all drained in the August 2008 image.

**Table 1:** Vital statistics of three supraglacial lakes identified on the surface of the Greenland Ice Sheet at Paakitsoq, where observed lakes match the position of modelled sinks on the DEM surface. Lakes H and J drain partially between the June and July LandSat images collected, while lake W increases its volume. All lakes drain by the collection of the August (11th) 2008 LandSat image.

**Figure 14:** Estimated surface lake volumetric evolution based on observed lake measurements, estimated lake depths, observed start of melt season date and assuming a constant filling/draining rate per day between the start of the melt season at Paakitsoq and the collection of the August 11th LandSat image where all three lakes had drained.

**Table 2:** Watershed details of the areas draining into each of the three lakes discussed above.

**Figure 15:** Trial run of the combined energy balance and surface routing models for an area of the Paakitsoq region (as defined in the previous sections of the present study), with modelled discharge at a pour point identified in the DEM surface for the

end of the melt season in 2007. Initial model results suggest that a substantial amount of modelled melt water does not enter the pour point.

**Figure 16:** Modelled discharge delivered to the pour point at lake *H*.

**Figure 17:** Lake *H* modelled volume.

**Figure 18:** Lake *H* modelled vs observed volume.

**Figure 19:** Modelled discharge delivered to the moulin at the base of lake *J*.

**Figure 20:** Lake *J* modelled volume.

**Figure 21:** Lake *J* modelled vs observed volume.

**Figure 22:** Modelled discharge at the pour point in lake *W*.

**Figure 23:** Lake *W* modelled volume.

**Figure 24:** Lake *W* modelled vs observed volume.

**Figure 1A :** Flow direction output visualized in ArcView 3.3, showing the flow direction of theoretical water inputs across the surface of the Paakitsoq region DEM used in the present study. Interpolation errors when the DEM was being created cause areas of the elevation model to exhibit uniform flow direction. In reality local topographic deviation at the sub-DEM resolution scale will cause small scale supraglacial flow variations that cannot be resolved by the static drainage routing function on such a coarse DEM, and thus uniform flow direction prevails.

**Figure 1B:** Supraglacial watersheds identified for the Paakitsoq region in ArcView 3.3. Areas corresponding to uniform flow direction exhibit large, anomalous watersheds due to the errors incurred in the DEM during the kriging and interpolation process (as discussed above). However, in these areas, only one sink was identified during ice surface static hydrological analysis.

**Figure 1C:** Watersheds identified for four lakes discussed above, as determined by the static supraglacial flow routing analysis. Surface areas were determined for each of the watersheds shown – lake H's watershed (pink) constituted 65.5 DEM cells, equating to 42.2km$^2$; lake J's watershed (blue) contained 19 DEM cells, with an area of 4.8km$^2$; lake W's watershed (green) is composed of 141.9 DEM cells, with an area of 35.5km$^2$.

**Figure 2A:** The first ice mask created to represent the ice margin at Paakitsoq (not including the Jakobshavn Isbrae glacier as the present study does not concern glaciers). The mask was created in Matlab R2006b software and the mask output illustrated is expressed in terms of 500mx500m DEM cells (134 rows and 161 columns of data).

**Figure 2B:** The second ice mask, representing the study area that contains numerous observed and statically modelled corresponding surface hydrological features. The extent of the modelled area is 1060km$^2$ (80 DEM cells by 53 DEM cells) compared to the initial 5393.5km$^2$ extent.

# 1. Introduction

The Greenland Ice Sheet has been studied regularly in recent glaciological literature as it provides insight into the dynamics of current and palaeo-ice sheets, and because of its potential global impact on sea level rise under a warming climate. The ice sheet is losing mass at an accelerating rate, from 50-100 Gt/yr between 1993 and 2003 and at even higher rates from 2003 to 2006 (IPCC 2007), and it has the capacity to raise global sea levels by >6.5m if the ice sheet were to melt completely (Gregory et. al., 2004). This catastrophic event is unlikely to occur (Oerlemans et. al., 2005), the consequences for low-lying regions worldwide are significant, and although in recent literature focusing on glacier dominated eustatic sea level rise, the contribution to sea level rise of the Greenland and Antarctic Ice Sheets have been ignored (Meier et. al., 2007), it is clear that ice sheets are important factors in sea level rise projections in the coming decades and centuries (Shepherd and Wingham, 2007). Recent research suggests that the Greenland Ice Sheet is capable of dynamic response to external forcing at relatively short time-scales to those even proposed by the most recent Inter-Governmental Panel on Climate Change report into the ice sheet (Bamber et. al., 2007). Further research into ice sheet dynamics and mass balance variations by Rignot and Kanagaratnam (2006) suggest that the rapid, dynamic response by the Greenland Ice Sheet to global warming may have contributed to the doubled rate of mass loss over the last decade (from 90 – 220$km^3a^{-1}$). The most recent research has suggested that ice sheet mass loss might be even higher (up to 262$km^3a^{-1}$ – Chen et. al., 2009), with two-thirds of this mass loss being accounted for by increased mass loss from outlet glaciers (ice dynamics), and enhanced runoff minus ablation accounting for the other third (Rignot and Kanagaratnam, 2006). Therefore understanding the influence of hydrological processes on ice sheet flow is important as proportionally ice sheet dynamics account for more of the variation in Greenland mass balance over the last decade than simply enhanced ablation due to global warming.

Observations near the equilibrium line of the western areas of the Greenland Ice Sheet have identified a positive correlation between increases in surface melting

induced by higher temperatures and seasonal ice sheet acceleration, where supraglacial meltwater was inferred to be routed through the ice sheet to provide basal lubrication for fast flow (Zwally et. al., 2002). Were a similar direct coupling mechanism to migrate to the margin and influence faster ice in outlet glaciers, McMillan and others (2007) suggest that this mechanism could cause further rapid dynamic response of the ice sheet to climate warming. Similar results have been obtained by Joughin and others (2008), although the authors identify that enhanced ice sheet flow by basal lubrication does only occur in the Greenland Ice Sheet interior, and thus is unlikely to lead to catastrophic ice sheet collapse. However, such enhanced flow is likely to affect the long-term stability of the Greenland Ice Sheet as the process causes ice sheet thinning (Parizek and Alley, 2004), and thus increases the surface area prone to ablation. An understanding of surface meltwater dynamics before this water enters the en- and sub-glacial hydrological system is needed to properly understand ice sheet dynamics as a whole, and how these dynamic processes vary over the course of a yearly accumulation and ablation cycle.

Further, an understanding of supraglacial melting and the subsequent flow and accumulation of this meltwater on the Greenland Ice Sheet surface is important in hydropower feasibility investigation. Hydropower in Greenland has the gross potential to provide 800,000 GW/h of energy per year (Ahlstrøm, 2007), and the Greenlandic Authority are investigating the possibility of hydropower supplanting the currently favoured diesel power plants – fifteen possible hydropower sites have been identified with the potential to generate 13,000 GW/h per year (Ice and Water Resources in Greenland website[1]), and the focus of much study into hydropower feasibility remains the generation of supraglacial melt (Ahlstrøm, 2007) and formation of supraglacial lakes on the Greenland Ice Sheet every year and how this water may be utilised in the production of 'green power'.

### 1.1 The present study

The supraglacial drainage system of glaciers and ice masses has been observed and noted by glaciologists such as Marston (1983), and later modelled by authors such as McMillan and others (2007), with much of this research focused on the Greenland

[1] http://www.iceandwater.gl/ - website last accessed 12.36pm BST, 9th May 2009

Ice Sheet because of the impact of the draining of supraglacial lakes on ice sheet dynamics. The present study seeks to investigate surface melting and routing of meltwater on the western margin of the Greenland Ice Sheet, around Paakitsoq, for the 2008 ablation season, by using a numerical model to investigate the inception and evolution of supraglacial lakes and by also using collected satellite imagery for the model study period to compare model results with actual observed supraglacial lake evolution. The present study also seeks to consider how effective the model is at producing results that are representative of measured observations

The model will produce meltwater hydrographs at a pour point (for example, a moulin at the base of a supraglacial lake basin) and by manipulating the output data, a volumetric analysis of model results will be conducted – assuming the pour point is ice-dammed (as is often the case with moulins at the beginning of the melt season on the ice sheet surface at Paakitsoq), it is possible to produce a graph of modelled supraglacial lake volume evolution throughout a melt season. This will be conducted for three lakes identified on the ice surface in 2008 whose locations correspond well with modelled sinks in the ice surface. These evolutionary graphs will then be compared to observed and estimated measurements of the actual supraglacial lake evolution on the surface of ice sheet at Paakitsoq.

The model does not actually deal with lake inception, evolution and drainage, rather the hydrographs produced suggest the rate of filling of lakes if the pour points are dammed. Thus modelled result comparisons with observed measurements are prone to difficulties when observed lakes drain and modelled results imply continuous filling. Model results will be discussed and the implications of model results on aspects of the ice sheet surface and subglacial hydrology will be highlighted. The accuracy and limitations of the model will also be discussed and compared to observations made from collected satellite imagery of the region during the 2008 ablation season. Conclusions regarding observed and modelled supraglacial lake evolution will be made while suggesting that more research into the development and testing of similar models could aid present understanding of these transient hydrological features that have the capacity to alter ice sheet dynamics substantially in a warming world.

## 1.2 Background

### 1.2.1. Supraglacial streams

Supraglacial streams are channels of flowing water incised into the surface of a glacier, ice cap or ice sheet by thermal erosion, and although their development is similar to that of alluvial or rock-based streams (Knighton, 1972; Kostrzewski and Zwoliński, 1995), rates of incision must exceed rates of ice ablation (Marston, 1983). These water-courses may be extremely diverse in their geomorphology, varying from location to location, and transport meltwaters from the outer limits of watersheds to a draining point – either off the glacier supraglacially, or via moulins and crevasses into the en- and subglacial environment (Stenborg, 1970; Knighton, 1972; Marston, 1983). Supraglacial stream regimes may be defined by meltwater (a nival regime), ablation water (a glacial regime) and by precipitation (a pluvial regime) inputs (after Kostrzewski and Zwoliński, 1995) and surface stream flow on the Greenland Ice Sheet is dominated by melt and ablation waters. These streams are devoid of clastic bank material and sediment, and experience discharge variations over short (diurnal) and longer (seasonal/annual) timescales (Marston, 1983; Kostrzewski and Zwoliński, 1995), although on the Greenland Ice Sheet, such streams are likely confined to the ablation season due to lack of meltwaters over the winter months. A 'long- term recovery' of water circulation routes is identified by Kostrzewski and Zwoliński (1995), suggesting that like supraglacial lakes (that form in similar locations every year on the Greenland Ice Sheet surface), supraglacial streams may recur with similar morphologies annually, or every few years. This recharging of relict surface drainage systems may be similar to recharge in en- and subglacial drainage networks found under the Greenland Ice Sheet and many other glaciers and ice masses worldwide (Jason Gulley, personal communication; Gulley and Benn, 2007).

Intra-seasonal variation in supraglacial stream flow is governed by rates of ablation – fluctuating hourly – and by the *Stenborg effect* (Stenborg, 1970; Kostrzewski and Zwoliński, 1995) where meltwater runoff is delayed by ice conditions and the porosity of the snowpack (Stenborg, 1970; Arnold et. al., 1996; Arnold et. al., 1998). Throughout the ablation season, supraglacial channels become wider as insolation receipts melt the stream banks more efficiently than stream-water thermal erosion of the channel bed (Kostrzewski and Zwoliński, 1995), and discharge into these streams varies depending on ice/snowpack conditions.

Thus supraglacial streams play an important role in providing supraglacial lakes with meltwater, and the rate at which supraglacial lakes fill is dependent on supraglacial stream dynamics. Further, 'spillover' (Marston, 1983) from supragalcial streams and lakes may cause discrete water courses and bodies to merge into larger homogenous areas and rapidly expand previously small supraglacial lake extents.

### 1.2.2. Supraglacial lakes

A supraglacial lake is a melt-pond of water on the surface of a glacier, ice cap or ice sheet (after Chikita and others, 1999). Supraglacial lakes form on Himalayan and Alpine glaciers, Icelandic and Siberian ice caps, polar polythermal glaciers and on the Greenland Ice Sheet (Ibid.; Luthje and others, 2006) during the summer melt season (Ibid.; Clarke et. al., 2005; McMillan et. al., 2007), but are unlikely to form on the Antarctic Ice Sheet due to the low temperatures, and lack of surface melting in the summer months (Benn and Evans, 1998).

Greenlandic supraglacial lakes have been identified since Weertman's (1973) research from the late 1960s into water-filled crevasse penetration from the surface to the bed of glaciers, while Zwally et. al., (2002) applied the same principle to the Greenland Ice Sheet and further investigated supraglacial lake distribution through the use of LandSat Enhanced Thematic Mapper (ETM) (Channel 3 – red spectrum of visible light) images to identify dark meltwater ponds (see figure 1) on the surface of the ice sheet in the Swiss Camp region of the western margin (north of Jakobshavn Isbrae) (Zwally and others, 2002; Long, MPhil dissertation).

Since this initial identification of supraglacial lakes using satellite imagery and geographical information systems (GIS) software, much recent research has focussed on determining the dimensions of supraglacial lakes on the Greenland Ice Sheet. Using MODIS (moderate-resolution imaging spectroradiometer) data, Box and Ski (2007) combined GIS-derived reflectance with raft-based measurements to determine the vital statistics of supraglacial lakes in Greenland's southwestern ablation zone from 2000-2005. Their results suggested the maximum area of an individual lake was 8.9 $km^2$ while the total volume of supraglacial lakes in this region reaches >1$km^3$ by July each year (Ibid). Further, lake dimensions may be in the region of hundreds of

meters in length, tens of meters wide, and over 12m in depth (Zwally and others, 2002; Box and Ski, 2007).

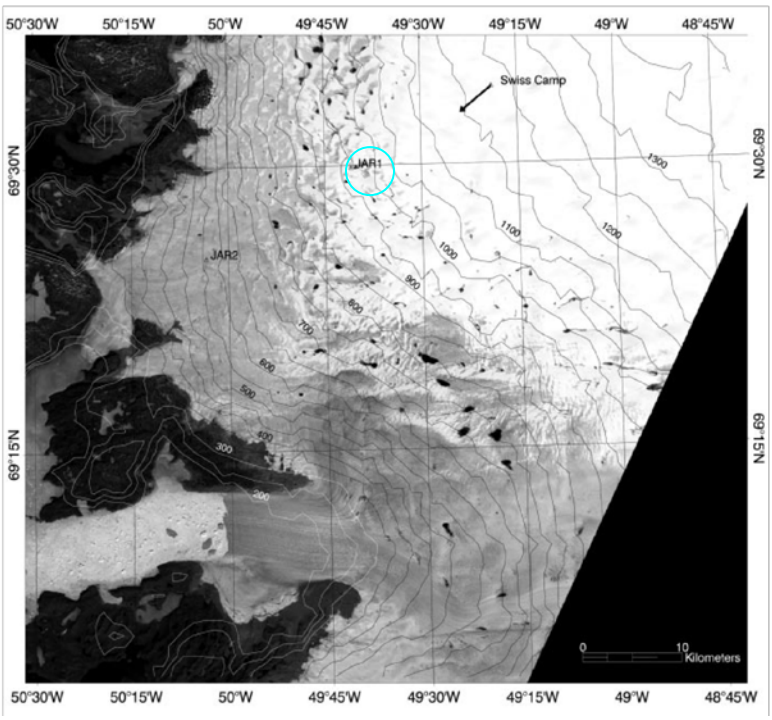


**Figure 1: LandSat ETM (Channel 3) image of the Swiss Camp region of the Greenland Ice Sheet surface. The image was taken on 22nd June 1990, typically one third of the way through the summer melt season. Melt ponds, or supraglacial lakes, are identified as black spots on the white ice background and may exhibit melt-water feeder or drainage channels. The location of the JAR 1 MET station is shown by the blue ellipse – MET data in the present study was obtained from this location. (Image reproduced from Zwally et. al., 2002)**

Although a wide range of lake sizes is apparent in this region of the ice sheet, large lakes normally occur no less than 10km from the ice margin (Thomsen and others, 1988) and are predominantly restricted to the inland ice above or near to the snow line (Ibid.; Long, MPhil dissertation). However, McMillan and others (2007) also suggest that the maximum elevation for formation of supraglacial lakes is around 1600m above sea level (with a typical elevation ceiling of 1500m).

Using 268 MODIS images from 2003, and the 2005-2007 melt seasons, Sundal et. al. (2008) investigated the seasonal evolution of Greenlandic supraglacial lakes and found that there is a 2-3 week delay between lake formation in northern Greenland compared to the southern and western regions studied. Further, the authors suggest that the onset of lake growth varies inter-annually, by up to one month, as lakes form and drain at progressively higher altitudes during the melt season (Sundal and others, 2008).

Analysis of 1978 and 1989 synthetic aperture radargrams of southwest Greenland by Jezek et. al. (1993) show stability between reflectors representative of lakes and other hydrological features over time, suggesting that they occur in similar, if not the same locations, every melt season. Analysis of a suite of hydrological

features on the surface of the Greenland Ice Sheet around the Paakitsoq region (Swiss Camp/Jakobshavn Isbrae) by Long (MPhil dissertation) from a LandSat image collected on 7th July 2001 and compared to Thomsen et. al's (1988) aerial photos from 1985 show that supraglacial lakes formed in similar regions (less than 200m apart) despite a 16 year time-lag between images. Further, various recent research on supraglacial lake evolution on the Greenland Ice Sheet has concerned lake drainage (Box and Ski, 2007; McMillan and others, 2007; Joughin and others, 2008; Das and others, 2008) and illustrates the transient nature of Greenlandic supraglacial lakes – figure 2 comprises four images collected in 2005 from a camera based at the JAR 1 MET station ('IceCam') to the north of Paakitsoq, and shows supraglacial lake inception, evolution and drainage over the course of 65 days in the ablation period.

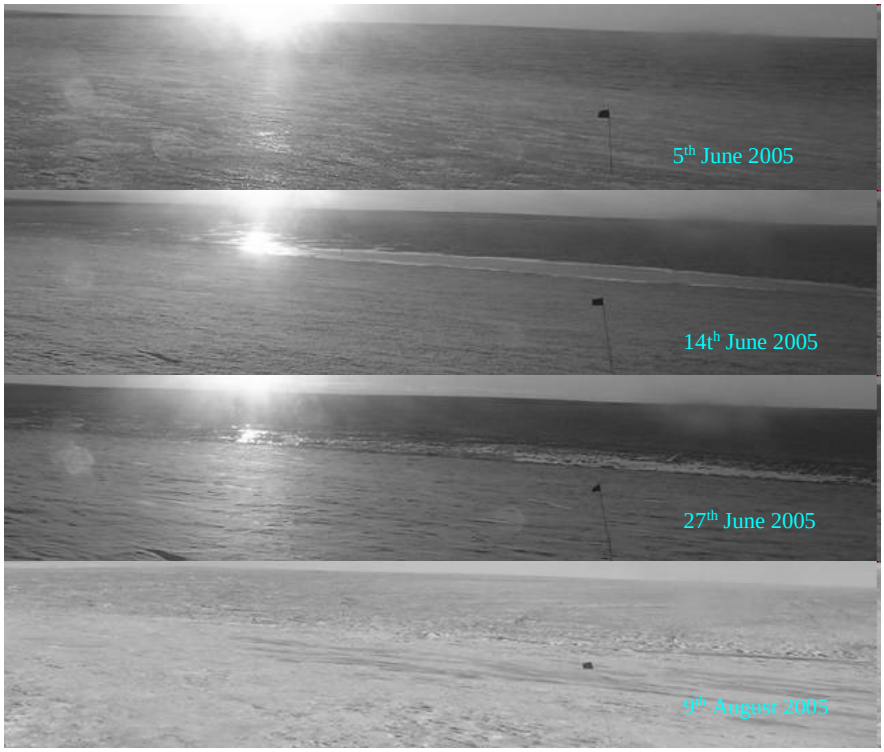


**Figure 2: Ice Cam photos showing the inception, evolution and drainage of a supraglacial lake at the JAR 1 MET station in the summer melt season of 2005.**

Thus supraglacial lakes on the Greenland Ice Sheet are ephemeral features, and although the melt ponds may form in similar locations in successive years, unlike those exhibited on Himalayan glaciers, they are unlikely to remain as continuous hydrologic features for more than one melt season (Watanabe and others, 1995; Wessels and others, 2002).

Supraglacial lake formation on the Greenland Ice Sheet occurs as summer ablation provides large quantities of surface meltwater. This meltwater flows on the

ice surface until it either drains into the ice sheet (via crevasses or moulins) or forms a surface melt pond (after Fountain and Walder, 1998). Such melt ponds may be debris-dammed like those on many Himalayan glaciers (Watanabe and others, 1995), but on the Greenland Ice Sheet, they exist in 'sinks' on the ice sheet's surface (after Long, MPhil dissertation) – sinks are depressions in the ice sheet surface (that are often identifiable on digital elevation model [DEM] GIS hydrological modelling functions, such as the DEMs manipulated in *ArcView GIS* software by Long [MPhil dissertation]). Sinks reflect possible entrances to the en- and subglacial hydrological system. These are normally crevasses or moulins that, over the course of the winter accumulation season, have filled with snow and ice and are dammed (Holmlund, 1988). Surface meltwater is routed across the ice sheet surface along hydraulic potential gradients (Marston, 1983) and then accumulates in the depressions of the ice-dammed crevasses or moulins (often seen as small very dark patches on satellite imagery – McMillan and others, 2007). These accumulating supraglacial lakes proceed to exert pressure on the ice dammed crevasses or moulins and may also cause limited melting of the ice plug (Marston, 1983; McMillan and others, 2007; Das and others, 2008), until the ice dam fails under a critical stress and melt water can percolate down the crevasse or moulin, probably penetrating to the bed of the ice sheet due to fracture propagation under high stress (Das and others, 2008).

Greenlandic supraglacial lakes are dynamic environments – they may take months to form, but have the capability to drain in a few hours providing up to $31.5 \times 10^6 m^3$ of meltwater in less than 24 hours to the ice-bed interface (Box and Ski, 2007). Feature tracking was used by Joughin et. al. (1996) to investigate clusters of lakes in September and October 1995 satellite radar interferograms around Ryder Glacier, northern Greenland, and suggested that the bare ice visible in October (compared to ice shrouded by meltwater in September) had actually collapsed due to lake drainage-induced fracture of the ice surface. This was most likely caused by a large volume of water draining very rapidly into the en- and subglacial hydrologic system (Das et. al., 2008). When combined with the data derived by Box and Ski (2007) from southwestern Greenland, supraglacial lakes may often contain enough water to locally hydraulically pressurize the subglacial environment upon draining, and cause various effects on the dynamics of the Greenland Ice Sheet (Joughin et. al., 1996; Zwally et. al., 2002; Box and Ski, 2007).

Research by Das and Joughin (2008) concerns the 50-100% speed-up of regions of the Greenland Ice Sheet upon drainage of supraglacial lakes at the heads of these regions – they suggest the complete drainage of a 5.6km$^2$ lake over twenty-four hours (with the majority of drainage in a ninety minute period) in the vicinity of Jakobshavn Isbrae in July 2006 caused a 980m vertical fracture from the ice sheet surface to the bed, and raised the ice sheet 1.2m within a few kilometers of the lake. Further, the authors suggest a 750m long block of ice was raised over 6m from the bed directly under the previously-submerged lake area, and measured velocities for the downstream extent of ice from the lake were 100% faster than those before the lake had drained (Das and Joughin, 2008). Meltwater inception to the ice sheet bed such as the 'Zwally hypothesis' concerning surface meltwater propagation, (after Zwally et. al., 2002) or the effects of lake drainage on the hydrodynamics of the Greenland ice sheet (Das and Joughin, 2008) only has an important influence on overall ice sheet dynamics, however, as it has a subdued or negligible effect on outlet glaciers, such as the Jakobshavn Isbrae to the south of Paakitsoq (Zwally et. al., 2002; Das and Joughin, 2008). This is because outlet glaciers have such high discharges and flow velocities, and are liable to more important and influential external forcing (such as the retreat of calving lines and ocean warming [Howat and others, 2007]). This conclusion is supported by Box and Ski (2007) who also suggest that if drained supraglacial lake meltwater is constrained laterally at the bed, water pressures will exceed the ice overburden pressure and lift the ice sheet locally over episodes of many hours, or even days, but that these effects would not be of high enough magnitude to cause significant variation in ice sheet elevation or flow anywhere other than on slow moving parts of the ice sheet.

Therefore supraglacial lake drainage events have the potential to rapidly supply water to the bed of the Greenland Ice Sheet. This may play a critical role in the linking of surface melt to ice dynamics (McMillan et. al., 2007) and thus the role that supraglacial lakes play in the hydrological cycle of Paakitsoq is of considerable interest, especially their inception and evolution, as this has been studied less extensively than their drainage. How supraglacial lakes store water, and then later release this water into the en- and subglacial hydrological system is important in the understanding of ice sheets hydrological cycles, and currently only a few runoff models allow for separate routing and delaying procedures for melt and precipitation in the glacier or ice sheet system (Jansson and others, 2003). The present study seeks

to investigate the storage component of supraglacial lakes to understand better their role in the Greenland Ice Sheet hydrological cycle at Paakitsoq.

### 1.3. The study area

The area of study is focussed on the Paakitsup Akuliarusersua basin at the Vestgrønland (Ilusisat) margin of the Greenland Ice Sheet. Paakitsup Akuliarusersua, more commonly referred to as Paakitsoq (Ahlstrøm, 2007), is a region extending inland from the ice sheet margin and located ~45km northeast of Jakobshavn, a town in the Disko Bugt (Figure 3).

Hinrich Rink was the first explorer/researcher to undertake fieldwork in the Paakitsoq region in October 1850 – he determined to make a map of the 'Indlandsisen' (inland ice), and his surveys started a series of data that has been accumulated over 150 years, with meteorological data first being recorded in Ilusisat in 1873.

However, it was not until the end of the Second World War that serious research expeditions to West Greenland began to provide scientific observations and data about the region. The Expéditions Polaires Francaises (1948-1953) and the Expédition Glaciologique Internationale au Groenlande (1957-1960) sought to investigate the profile of the ice sheet from East to West (ending

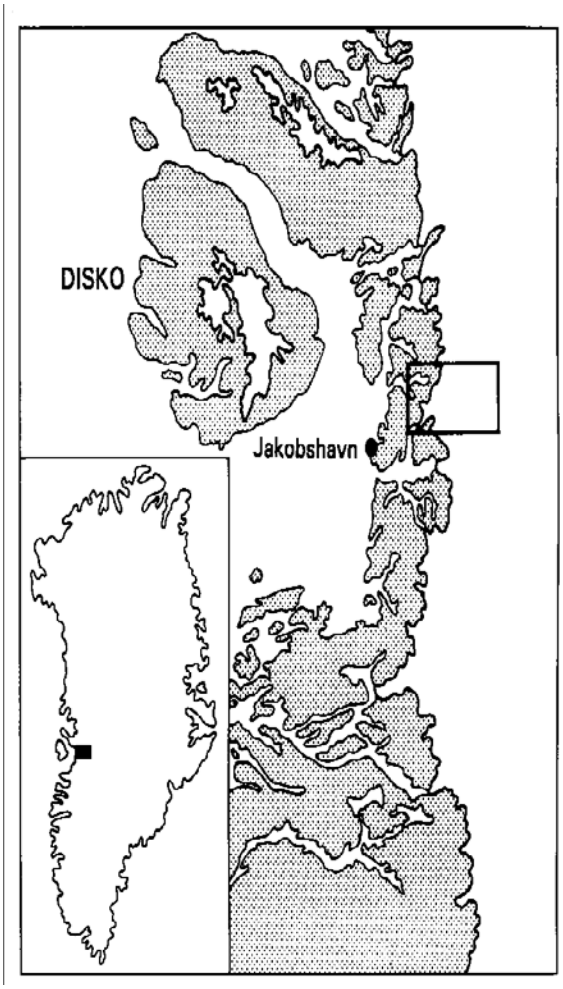


**Figure 3: The study area in Greenland (identified by a rectangle).**

near the Disko Bugt), and then photogrammetarilly map outlet glaciers in the Ilusisat region respectively, while from the 1970s, pre-feasibility investigations into hydropower have expanded research interests in the region (www.geus.dk – Ilulissat Icefjord; Ahlstrøm, 2007).

Such pre-feasibility investigations into the possibility of harnessing the vast quantities of water available in Greenland were mainly concerned with utilising en- and subglacial meltwaters, rather than supraglacial lakes, and it wasn't until the very end of the Twentieth Century that glaciological interest in the Greenland Ice Sheet began to increase and focus research on ice sheet mass-balance, hydrology and dynamics (Ahlstrøm, 2007). Led by research organisations such as the Greenland Survey (ASIAQ), formerly known as the Greenland Technical Organisation (GTO), and Geological Survey of Greenland and Denmark (previously GGU, now GEUS), studies of Greenland Ice Sheet mass balance and ice temperature, supra-, en- and subglacial hydrological regimes and ice-sheet dynamics, and investigations into the ice and bed topography (including mapping, production of digital elevation models – DEMs – and feature tracking) have been undertaken (Ahlstrøm, 2007).

An extensive study of the regions glaciology and hydrology was conducted by Thomsen and others (1988), identifying a dynamic surface hydrological regime and morphology on the inland ice at Paakitsoq: supraglacial lakes litter the ice surface, with lengths ranging from a few tens of meters to nearly two kilometres, and often connected, or fed by surface meltwater channels. Average lake depths were given as between c.2-5m with a temperature profile that remained constantly positive within the lake depth-profile (with lake temperatures normally between ~0.1-1°C – Thomsen and Reeh, 1986, as cited in Long, MPhil dissertation). As identified by Thomsen and others (1988), the supraglacial lakes on the ice surface at Paakitsoq often drain (a trait commonly exhibited by ice-marginal Greenlandic surface lakes – Ahlstrøm, 2007), revealing moulins or crevasse-like features into which the lake water has flowed, with average moulin diameters of 1-2m (Thomsen et. al., 1988), and an aerial moulin density of c.0.2 $km^{-2}$ identified by Zwally and others (2002) during their hydrological investigations of surface melt-induced acceleration of the Greenland Ice Sheet. A small flux of surface meltwater (or discharge per unit area per unit time – Colbeck, 1972) may leave the ice as marginal runoff, but most is entrained in the supraglacial hydrological regime and enters surface channels and lakes, to later enter the en- and subglacial hydrological system upon lake drainage.

Further investigations into the areas supraglacial hydrology have been conducted by McMillan and others (2007), who investigated the seasonal evolution of supraglacial lakes on the ice sheet surface in the region around Paakitsoq and Swiss

Camp, Luthje and others (2006), who used a one dimensional model to investigate the melting of the ice surface and the ice surface under a supraglacial lake, and Box and Ski (2007) who used remote sounding to investigate the vital statistics of various surface lakes to the north and south of the Jakobshavn Isbrae.

# 2. Methods

## 2.1. External data

*Ice surface elevation*

A DEM of the ice surface at Paakitsoq was procured from GEUS (Ruth Mottram and Andreas Ahlstrøm, 2008, *unpublished data*). The DEM was created using an airborne LiDAR (Light Detection and Ranging) scanning module, capturing ice surface elevations on a series of specified flight paths. One of the flight paths is shown in Figure 4, and covers both inland ice and non-glaciated areas of the Disko basin.

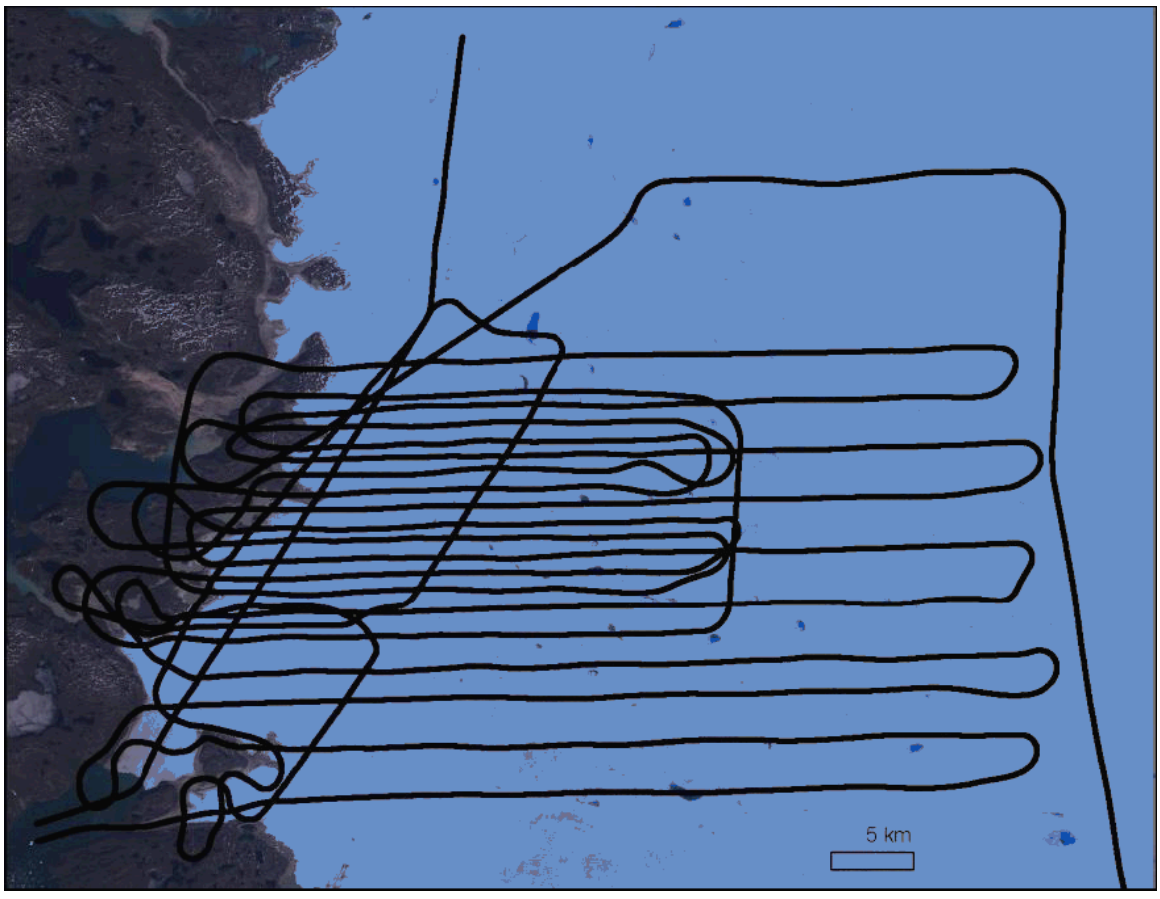


**Figure 4: The flight lines used to collect LiDAR data in the study area, from one of the data collection flights.**

The data collected from the LiDAR survey were uploaded into Golden Software's Surfer program and interpolated using the geostatistical linear kriging technique. On interpolation, an ice surface elevation DEM was produced with a resolution of 500m.

*Meteorological data*

Meteorological (MET) data were recorded by the JAR1 GC-NET automated weather station (AWS), located at 69° 29‟ 54" N, 49° 40‟ 54" W (Steffen et. al., 1996). The data employed by the energy balance and supraglacial routing submodels relate to humidity, air temperature, wind speed and direction, snowpack thickness and albedo, and these data were obtained from the Steffen Research Group's *Greenland Climate Network (GC-NET)* (http://cires.colorado.edu/science/groups/steffen/gcnet/). The data provided by GC-NET covered the period from September 2007 – August 2008 and is the latest publicly available data sequence for the Paakitsoq region (Konrad Steffen, personal communication, 7/4/2009). Precipitation data are not available for the region (Steffen and Box, 2001) and thus the model is run with no extra precipitation input (using just water equivalent of snowpack thickness and the surface energy balance model to melt the snowpack and create surface meltwater) – this is unlikely to influence model results as this region of the Greenland Ice Sheet experiences a regional climate that is dominated by Icelandic cyclones which are not favourable for precipitation over the ablation season (Chen et. al., 1997) when the model produces its results for supraglacial lake meltwater inputs.

*Satellite imagery*

Images were downloaded from the United States Geological Survey (USGS) *Earth Explorer* website: http://edcsns17.cr.usgs.gov/EarthExplorer/[2]. The LandSat-7 Enhanced Thematic Mapper (ETM) images have a 30m pixel resolution, and were downloaded for the 24th June, 26th July and 11th August 2008.

After 31st May 2003, all LandSat-7 ETM images are subject to 'stroking', as Scan Line Corrector (SLC) failure occurred on the satellite on this date. Thus the images downloaded for this study are 'SLC off' and contain data gaps often from the

[2] Website last accessed 2nd June, 2008, 6.29pm BST.

image margins where no image can be recovered. However, in the present study, the lakes of interest (that correspond with sinks in the DEM surface) fall in areas that are not affected by the SLC failure and the lake extents are often clearly identifiable. Those lakes that are not easily identifiable due to SLC-off interference are reconstructed through automatic identification and interpolation within ERDAS Imagine software.

### 2.2. Manipulation of data

The numerical model requires an hourly time-step input of meteorological data. The data available from the Steffen Research Group's GC-NET website often contained errors that needed removing from the dataset – the holes created in the data then needed to be filled with accurate, interpolated data so the model could be run effectively.

The MET data were collected by AWS and although data collection remained continuous throughout the study period (Steffen et. al., 1996), during the incredibly cold winter months the MET station failed to record actual meteorological data and 'jammed', recording repeated measurements over many hours or days. These data errors were recorded in the air temperature, relative humidity and wind speed data and different techniques were employed to correct for these data errors.

*Air temperature data*

Uploading the air temperature data in statistical mathematical computer packages (Microsoft Excel 2008 and Matlab R2006b), graphs were plotted of the dataset and first degree polynomial trend lines were fitted to visualize the seasonal trends in the air temperature at Paakitsoq. Where data were unavailable, such as between 2930-5930 hours, the data were interpolated using the polynomial equation:

$$y = 8\text{E-}07*x^2 - 0.0076x - 2.9646$$

where $y$ is air temperature and $x$ is time from the beginning of the dataset used in the model run. Although this data interpolation gives an estimate of the air temperature at

a given time, based on the trends of collected data, it does not account for diurnal fluctuation in air temperature at Paakitsoq. Thus model runs incorporating this part of the dataset are likely to exhibit subdued surface melting compared to where actual air temperatures are available.

*Relative humidity*

Data were erroneous in the relative humidity dataset in seven segments varying from five hours of missing data to over nine-hundred hours (between 3800-4750 hours). Data gaps were interpolated by using the polynomial equation:

$$y = -2E\text{-}07*x^2 + 0.002x + 82.088$$

(where $y$ is the relative humidity and $x$ is the time from the beginning of the dataset used in the model run) given when the dataset was presented in a statistics package (Microsoft Excel 2008) and visualized in graph form. Similar to the interpolation of the air temperature dataset, this provides a seasonal trend within interpolated data, and although it does not allow for diurnal fluctuation in relative humidity, this lack of diurnal fluctuation may be overlooked (as it may be with air temperature interpolation) as the spread of data is extensive and representative of the regional climate characteristics (after Kosiba and Loewe, 1964).

*Wind speed and direction*

The dataset collected by the AWS for wind speed and direction contained a minimal number of non-recorded hourly steps. Data gaps were only of a maximum of two consecutive hours, and gaps were filled manually by taking an average of the previous and next wind speeds/directions recorded in the data series. For example, a data gap preceded by a windspeed recording of $1.4ms^{-1}$ and superseded by a windspeed recording of $1.6ms^{-1}$ was interpolated as a windspeed of $1.5ms^{-1}$.

*Snow depth*

Snow depth data were recorded at the MET station only. The numerical model requires initial snow depth data across the whole of the study area (each DEM cell used in the model runs), not just at one point. The first successful

model run was conducted by taking the average of the snow depth recorded by the AWS in the first ten days of the available dataset (in early September 2007). This depth measurement was then converted to snow water equivalent (SWE) input needed to run the model, using the following formula (from Maurer, Masters Thesis):

$$\text{SWE (in mm.yr}^{-1}\text{)} = \text{depth of snow layer (cm) x average snow density (g.cm}^{-3}\text{)} \div \text{density of water (g.cm}^{-3}\text{)} \times 10$$

where the average snow density is 0.33g.cm-3 as derived by Krabill and others (2004) for the region, and the density of water is 0.1g.cm-3. The SWE given by the formula was then converted to meters.

Further model runs were conducted after the initial successful model run, and utilised a more realistic value for the snow depth than at the end of the 2007 melt season. In their study into determination of snow grain sizes, Painter and others (2007) dug snow pits at Swiss Camp (just to the north of the present study region) and found that at the very beginning of the melt season (in mid-May), the snow depth was ~2m before the onset of summer melting. This is confirmed by examining the available snow depth data (on May 1st 2008, snow depth was recorded at 2.16m at JAR1 AWS). A value of 2m was chosen to represent the overall snow cover across the entire DEM extent used in the model runs as the amount of extra precipitation that occurs with increased elevation is not known at Paakitsoq (Maurer, Masters Thesis), and is unlikely to mean that there will be a shallower snowpack at elevations higher than the lowest extent of the DEM used. This snow depth was converted to SWE (2m of snow equates to 6.6m.yr-1 SWE) and data was inputted into the model.

### 2.3. Modelling and analysis

2.3.1. Static drainage system analysis

The supraglacial drainage system across the inland ice at Paakitsoq was investigated through a static analysis in ArcView 3.3 (ArcGIS 9.2) software, using the Spatial Analyst extension. The hydrological modelling function was employed, and a detailed description of the analysis tools used in the software is given in Appendix A. Supraglacial melt routines were visualized using the raster-based D8 SFD (single flow direction) routing model (applied previously by Arnold et. al., 1998, to Haut Glacier d'Arolla, for example). The D8 SFD routing model assigns each cell in a surface

DEM a flow direction related to the neighbouring pixel with the steepest downslope gradient (Kenny and Matthews, 2005), and allows for a maximum 8 flow directions. Sinks in the surface DEM were identified and their locations were compared to actual lake locations from the satellite images procured for 2008. Further analysis was conducted to identify supraglacial 'channels' of high flow accumulation, by calculating the number of upstream cells draining into each cell, and watersheds for discrete surface features (such as lakes) were determined by calculating every cell that contributed supraglacial discharge to the given sink. Appendix A describes the extended methods adopted in the static drainage system analysis.

### 2.3.2. Surface energy balance model

A distributed surface energy balance model was used (after Arnold et. al., 1996) to calculate hourly variations of water input into each DEM cell (Arnold et. al., 1998). Rainfall was not measured at the JAR GC-NET MET station although as summer ablation rates are likely to exceed precipitation inputs by orders of magnitude (Steffen and Box, 2001), the lack of rainfall input will not influence the supraglacial lake input hydrographs excessively.

The model uses a DEM of the ice surface, known start of season snow depth data, and known meteorological data to calculate the surface energy balance of each DEM cell (Arnold et. al., 1998). The surface energy balance of the ice surface is calculated from the sum of the net shortwave (SWR), net longwave (LWR), sensible heat (SHF) and latent heat (LHF) fluxes (shown in equation 1), with the component relating to insolation being treated in most detail, as solar radiation is acknowledged to be the greatest source of melt energy (Oerlemans, 1993).

$$ABL = SWR + LWR + SHF + LHF$$

[Equation 1: the energy balance model assumes four significant energy flux components at the ice surface determine ablation rates. All contributing components are expressed with units of mm of water per unit time. Further equations relating to the determination of radiative heat fluxes and turbulent heat fluxes can be found in Arnold et. al., 1998.]

The surface energy balance model also takes into account of the effects of aspect and shading by surrounding topography, and glacier surface slope, on insolation receipts, although this sub-routine is unlikely to be employed on the inland ice of Paakitsoq (Neil Arnold, *personal communication,* 9th April 2009), apart from around relict or in-use sinks and channels in the ice surface created by meltwater incision or ice fracture (as described by Marston, 1983). A shading frequency of '1' was employed for all model runs. Further, the model includes an empirical relationship for the changing surface albedo depending on the removal of the winter snowpack, or the fall of new snow (as detailed in the MET data model input). Using Oerleman's (1992, 1993) relationships, albedo was calculated for the energy balance model using empirical parameters that were derived from in-situ measurements taken at Haut Glacier d'Arolla, Switzerland, by Arnold and others (1996, 1998). Although unlikely to be identical to the albedo of Paakitsoq, the albedo relationship within the model remains a good estimate of glacier ice in general and is unlikely to affect model outputs unduly (Neil Arnold, *personal communication*, 9th April 2009).

### 2.3.3. Supraglacial melt routing model

Using the meltwater output from the surface energy balance model, and known precipitation over the study area, data was inputted into a supraglacial routing model (after Arnold et. al., 1998). The model allows individual moulins or 'sinks' to be identified and their drainage basin established, with an algorithm estimating the time taken for water to flow from each DEM cell to a given sink. The model assumes that water flows from one cell to the next adjacent cell down the steepest slope (following the D8 SFD method adopted in ArcGIS software)[3], and accounts for the delay of vertical and lateral movement of water through the snowpack (Willis et. al., 2002) as suggested by Colbeck's equations of water flow through snow (1978, as cited in Chow, 1978).

[3] The author recognises that in reality, supraglacial water flow along an ice sheet does not occur by simple downslope transmission, rather it follows the hydraulic potential of the ice surface (Paterson, 2000). However, addition of this aspect of water flow into the numerical model would be of limited help to the accuracy of model outputs considering initial analysis of data in ArcGIS software followed the D8 SFD method included in the software package.

The first of Colbeck's (1978) equations used in the routing model concerns the vertical flow of water in unsaturated snow, for all DEM cells with snow cover at a given time:

$$D = \kappa_e d/(3\rho_w g/\mu)^{1/3} k^{1/3} q^{2/3})$$

where *D* is the time taken for water to percolate vertically through the snowpack (in seconds). The other parameters are as follows: $k_e$ is the snowpacks effective porosity (0.63), *d* is the snowpack depth (m), $\tilde{n}_w$ is the density of water (kg $m^{-3}$), *g* is acceleration due to gravity (m $s^{-1}$), ì is the viscosity of water (Pa s), *k* is the snows permeability (6 x $10^{-9}$ $m^2$) and *q* is the flux of water through the snowpack. This flux is the water inputted into the model previously generated by the surface energy balance model, plus liquid precipitation ($m^3$ $s^{-1}$) from the MET data. Constant values of snowpack porosity and snow permeability were adopted. Although these parameters could be measured in the field, albeit with difficulty, they change with time during the melt season, and represent micro-scale snowpack evolution physics that go far beyond the capacity of this project (Arnold et. al., 1998).

The second equation used in the model concerns the flow velocity of water in a saturated layer at the base of a snowpack, across a snow covered DEM cell:

$$C_s = (\rho_w g/\mu) k\theta/\kappa$$

where $C_s$ is the velocity of water under a snowpack (m $s^{-1}$), *è* is the surface slope, and k is the snow porosity (Colbeck, 1978, in Chow, 1978). For both of Colbeck's equations given above, the values used in the present study are for 'medium grain old dry snow' (from Male and Gray, 1981, p.401, as cited by Arnold et. al., 1998) as this is likely to reflect the inland ice condition.

Where DEM cells exhibit an icy surface, water flow velocity on ice (*C*i) is dealt with using Manning's equation:

$$C_i = R^{2/3}\theta^{1/2}/n$$

where *R* is the hydraulic radius of the supraglacial channel (m), and *n* is the Manning roughness coefficient ($m^{-1/3}$ s). A constant value for *R* is assumed (0.035m) because of

the high roughness of the ice sheet surface, and because of the rapidly changing nature of the ice surface during the ablation period. This adoption of a constant value has little effect on sink input hydrograph form compared to the presence (or absence) of snow cover in a sink catchment.

The time taken for water to cross each snow or ice covered DEM cell can therefore be calculated by using the above equations. The sum of all individual times for each cell on all paths (between a melt source cell and the relevant sink cell), including the vertical percolation time through the snowpack can then be calculated to give the total time taken for each hourly melt/rain increment to reach each sink (Arnold et. al., 1998; Willis et. al., 2002). Sinks in the DEM surface develop individual input hydrograph shapes dependent on the shape of the basin draining to the sink, and also on the snowpack condition (or lack thereof) in the basin.

### 2.3.4. Full system model runs

The model experienced initial teething problems when run with the whole DEM extent, and failed to complete its routine. However, when run with a single DEM cell input, the model calculated melt at a pour point off the cell, which suggested that the model could not deal effectively with the mountainous topography (namely ridges) that was not covered by the ice sheet when run at full DEM extent (Neil Arnold, *personal communication*, 2nd June 2009). A rough 'cut' of the DEM was therefore created (representing the ice extent, from margin to the limit of the inland ice extent) so that the model could be run with the full ice extent provided by the DEM, but exclude the mountainous topography at the ice margins. The model also failed to complete its routine when this 'cut' was employed. It was then decided to create a second 'cut' of the DEM, concerning an area identified in the LandSat imagery (for 2008) that exhibited a suite of hydrological features that corresponded well with surface sinks visualized in the static supraglacial routing analysis (employed in ArcView 3.3 GIS software). The model ran successfully with an hourly timestep for a period of 50 days with meteorological data from the end of the 2007 melt season, and thus the second 'cut' of the DEM was accepted as the subsequent topographic model inputs. The initial DEM image and subsequent cuts are visualized in Appendix B. The hydrographs produced in the first successful model runs provide valuable insight into the resolution of the model and how it deals with predicted and

observed trends in surface meltwater production, and are discussed in the results section. The DEM 'cuts' are given in Appendix B.

After correcting for the model failing to complete its routines, the topographic extent of the DEM is much more limited than the LandSat imagery, and covers a section of the inland ice to the north east of the Jakobshavn Isbrae. The study area in the present investigation still remains as that covered by the whole of the DEM provided by GEUS, however, as it is possible to draw conclusions in the present study into supraglacial lake evolution on the Greenland Ice Sheet at Paakitsoq from the LandSat imagery alone (in areas such as the ice margin), and then draw upon the more extensive results that are produced by the numerical model for a more focussed region of the study area (that has bee identified as containing a wide range of clearly visible hydrological features). Thus the limited DEM extent used in the model does not affect the accuracy of the results in the present study.

# 3. Results

## 3.1. Observed features

Suitable satellite images were not available covering the Paakitsoq region at the start of the melt season, due to the presence of cloud, but in the first image available from the 24th June 2008 (figure 5), a suite of hydrological features are already visible on the surface of the ice sheet. Blue features are identified as supraglacial lakes. A wide range of lake sizes is evident, with larger lakes up to c.2km long, and c.1km wide and much smaller ponds as small as only a few tens of meters across. There are many different sizes and shapes of lakes in between these extreme dimensions, although large lakes typically evolve no less than 10km from the margin of the ice sheet and are often restricted to the inland ice near to, or above the snow line (Thomsen et. al., 1988; McMillan et. al., 2007), while smaller lakes may form in almost any location on the ice sheet. Two large lakes are identified as being almost completely ice-capped (by surface floating ice), while further small lakes have partial ice-capping. A high concentration of large lakes is found between 900-1000m above sea-level, with few lakes occurring above this elevation. In the 24th June image, a series of surface streams are also identified. Occurring like the lakes at distances of over 10km from the ice margin (although most large streams are present at least 20km

from the margin), such supraglacial streams appear to drain some lakes and feed others. The visible streams are often sub-parallel (Marston, 1983), although the largest supraglacial channel arcs between two small lake extents – interestingly, Kostrzewski and Zwoliñski (1995) suggest that the dimensions and characteristics of supraglacial streams still often remain contentious and under-defined, and therefore this arcing surface channel could also be considered a highly sinuous supraglacial lake by these authors' definition, although in this image it appears to be only 85% filled compared to the channels identifiable maximum extent.

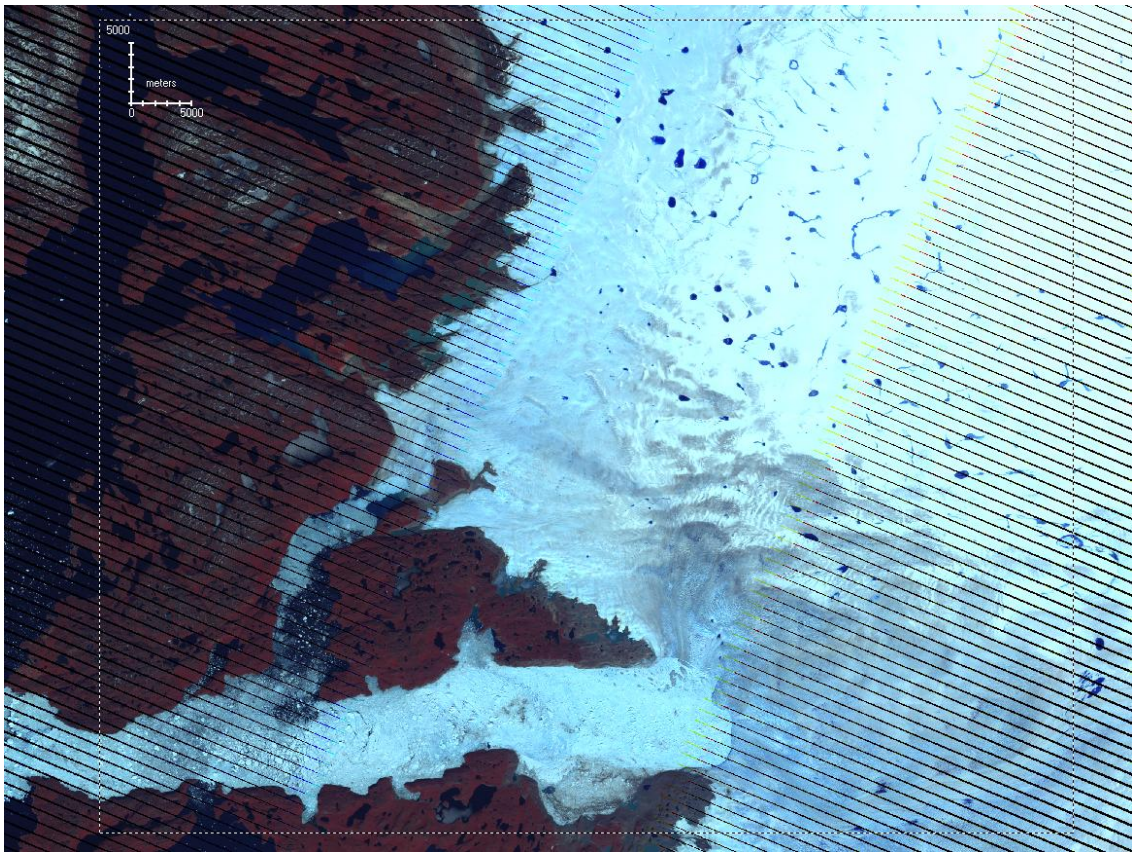


**Figure 5: LandSat image of the Paakitsoq region, collected on 24th June 2008. Inside the dotted rectangle is the present study area (where DEM coverage is available). Supraglacial hydrological features such as lakes and meltwater channels are clearly visible as dark blue shapes on the lighter blue/white ice surface. Large lakes typically form more than 10km from the ice margin, as shown in the image.**

Such surface hydrological features have been identified previously in supraglacial hydrodynamical studies of the region, and the features visible in the 24th June 2008 image are consistent in formation, location and dimension to the suit of hydrological features identified by Thomsen and others (1988) from aerial photographs taken in 1985, and later re-identified by Long (MPhil dissertation) from

satellite images collected in 2001. The single hardest features to identify in the 24th June 2008 image are individual moulins or crevasses (that are ice-dammed and thus allow supraglacial lakes to form at the beginning of the melt season). This is because typical moulin diameters in the Paakitsoq region (of c.1-2m according to Thomsen et. al., 1988) fall well below the resolution of LandSat-7 ETM images (with a resolution of 30m). However, as in Long's (MPhil dissertation) analysis of 2001 satellite images, large black spots between c.50-200m across are sometimes visible beneath light blue supraglacial lake extents, or even on the bare inland ice surface of the 24th June 2008 image. The Paakitsoq region has a moulin density of 0.2 moulins per square-kilometre (as calculated by Thomsen et. al., 1988) and therefore the anomalous black spots amongst the light blue supraglacial lake or white ice surfaces are considered to be moulins, crevasses or morphologically similar phenomena similar to, and associated with englacial drainage entrances (Das et. al., 2008).

A second LandSat image collected on 26th July 2008 shows change on the inland ice surface – many of the small lakes littering the surface of the ice sheet below 900m above sea level have drained, as have all but two of the large lakes between 900-1000m elevation, often leaving behind darkened patches on the ice surface that indicate their former basin location and maximum dimensions. This is similar to the results indicated by McMillan and others (2007) in the same region. However, a large number of lakes have formed at higher elevations (above 1000m above sea level) in the study area. The sub-parallel supraglacial streams also appear to have drained, although they leave darkened relict channels that are clearly visible in similar locations to the filled channels identified in the 24th June image, as shown in figure 6.

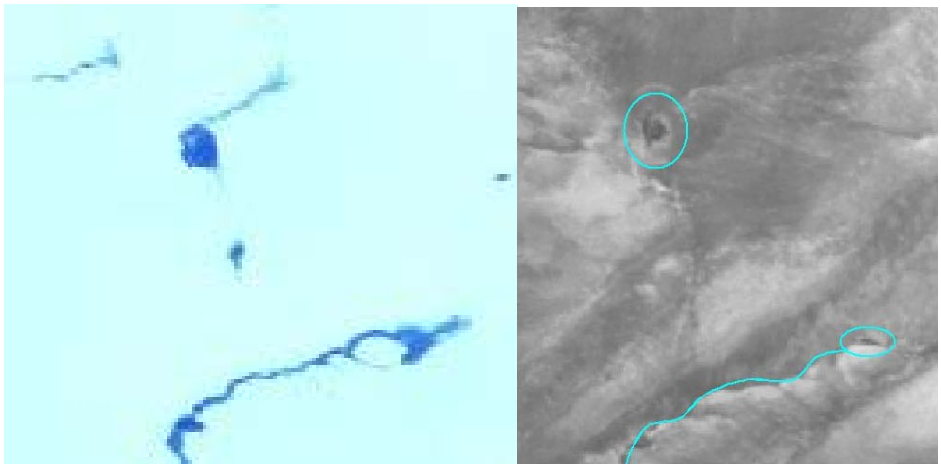

**Figure 6: Left – surface lake and stream morphology on 24th June 2008; right – relict lake basin (top ellipse) and relict lake basin with relict drainage channel (bottom ellipse and line) on 26th July 2008. The relict lakes are clearly visible as darkened patches on the ice surface, while the supraglacial stream channel is identifiable as a darkened sinuous line on the ice. At increased zoom, the right image showing relict lake basins shows a very dark agglomeration of pixels in the upper highlighted lake bed – this is interpreted to be a moulin or crevasse into which the lake water drained between 24th June and 26th July 2008.**

Further dark surface channels are identifiable that are not visible in the earlier June 2008 image, which implies that in the preceding month to the July image being taken, more surface channels were filled on the ice sheet surface, but have then drained before the image was collected. This illustrates the ephemeral nature of the supraglacial hydrological system at Paakitsoq and how, in the space of 32 days, previously filled surface lakes and channels can drain and leave only relict channel and depression morphologies. As in the study conducted by Long (MPhil dissertation), some of the lake basins that had drained between 24th June and 26th July often exhibited dark blue or black patches or spots at the base of the basin extents which are interpreted to be moulins or crevasses into which the lake water drained (such as the lake basin that is shown in figure 6 above), as has previously been proposed and investigated by authors studying Paakitsoq (Thomsen et. al., 1988; McMillan et. al., 2007) and other comparable glaciological environments (Boon and Sharp, 2003; Mernild, 2006).

A third LandSat image collected on the 11th August 2008 shows further supraglacial lake and stream drainage, with only a handful of very large lakes (some over 2.3km long) visible at above 1100m elevation, and no identifiable supraglacial streams. This concurs with the results given in McMillan and others (2007) who suggested that by August, 95% of surface lakes were found above 880m, with a great increase in total lake area above 1200m (between images taken in July and August). Relict lake and channel depressions are visible from in similar locations to the remaining July 2008 image lake extents, although further surface meltwater channel evolution is visible between the July and August images, suggesting that the supraglacial hydrological regime of Paakitsoq is still as dynamic as the region was in 2001 when investigated by McMillan and others (2007), and over a decade before this (when mapped by Thomsen et. al., 1988) – further, the suite of hydrological features that are identified in Thomsen and others' map (1988) are only offset c.300m with the same features identified by Long (MPhil dissertation) in 2001, and by the present study in 2008.

Figure 7 shows Thomsen and others map of part of the Paakitsoq region, with a LandSat image from 7th July 2001 superimposed upon it (both have been georeferenced), while the light-blue ellipses and lines show the position of three of the lakes identified in the map and 2001 LandSat image that also occur in the 24th June 2008 LandSat image, along with two identifiable surface channels surrounding two of

the lakes. The larger of the three lakes is not offset from the lake identified in 2001 by Long (MPhil dissertation), and is only c.200m from the dry lakebed mapped by Thomsen and others (1988). The two smaller lakes are also not offset to the lakes identified in the 2001 LandSat image, and the two supragalcial streams associated with these lakes correlate well, if c.100m offset, with a series of surface channels mapped in the region by Thomsen and others (1988). The main difference between the large lake identified by Long (MPhil dissertation) and in the present study is the lack of ice-capping in the 2008 image, and that the lake appears to be substantially smaller in dimension compared to the 2001 extent, probably due to the difference in date of the LandSat image collection (the 2001 image being taken in July and the 2008 being taken in mid-June, and thus the lake has had less time to fill during the melt season).

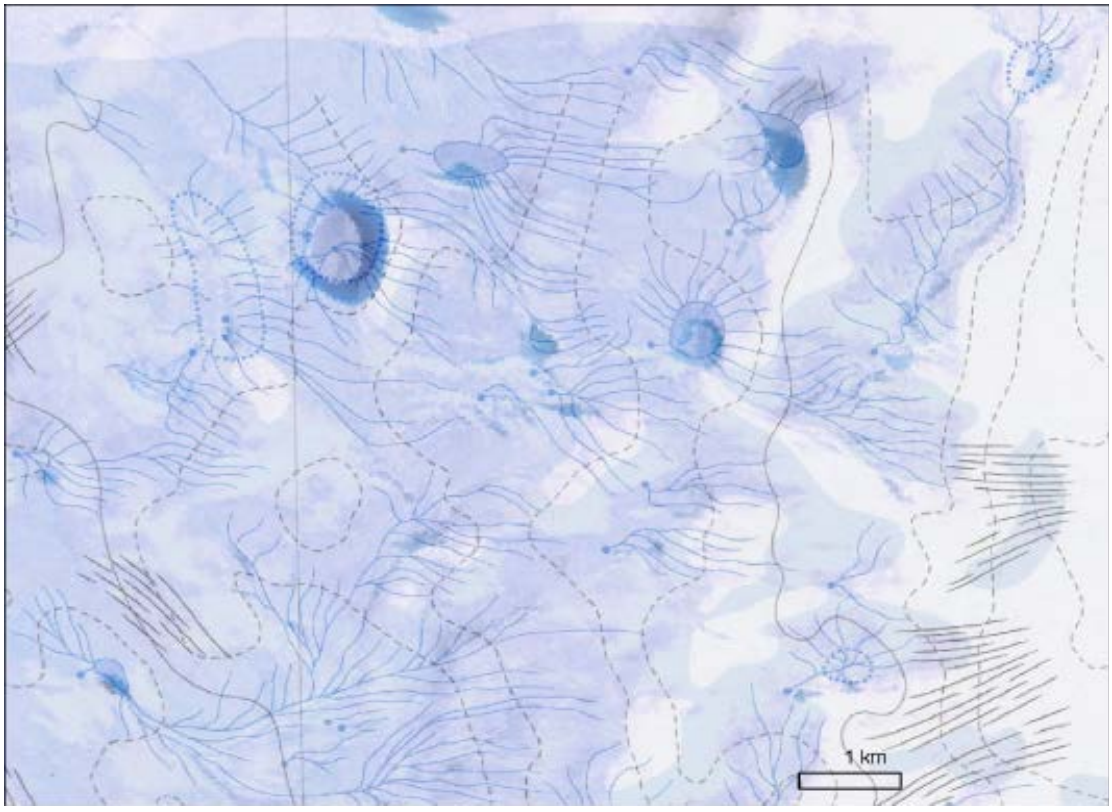


**Figure 7: Supraglacial hydrological features at Paakitsoq, showing Thomsen et. al.'s (1988) map, 1st July 2001 LandSat image (taken from Long, MPhil dissertation) and the position of three lakes from 24th June 2008 LandSat image with two surface channels associated with the lakes (in light blue). The region has been chosen because of the correspondence of features in the three datasets, despite a twenty year difference between first and last data collection.**

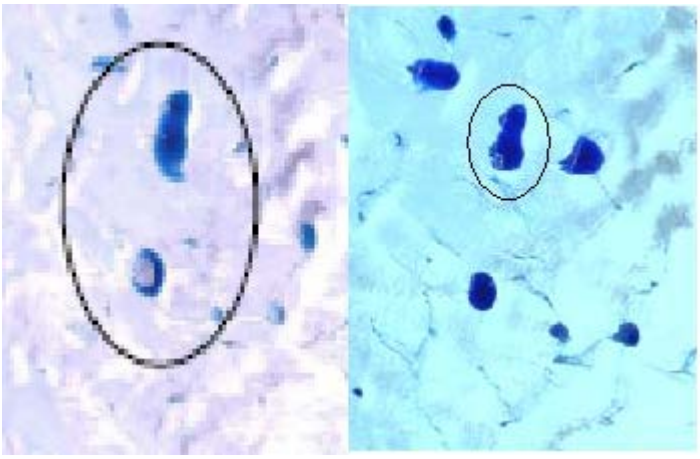

**Figure 8: Left – July 7th 2001 image showing the extent of two lakes; right – June 24th 2008 image showing the extent of the same identified lakes. The circled lake in the right image corresponds to the top lake in the left ellipse image and has shrunk in extent between the two dates (although as these dates are 'snapshots' into the evolution of the lakes, the right-hand lake may still have filled later in the melt season to the 2001 maximum extent).**

This variation in lake volume (of the large lake shown in figure 7) is mirrored by the more substantial lake to the north as shown in figure 8 – in 2001, the lake extent appears to be greater than in 2008, and this is confirmed by the availability of an elevation profile across this lake taken from the 2001 flight lines (figure 4). In 2001, the local maximum lake depth was 9-10m (derived from the flight line passing close enough to the centre of the lake for the figures to be interpreted as a reasonable estimate of the lakes actual dimensions) with an average depth of 5.1m (Long, MPhil dissertation). These figures enable a rough estimate of the volume of water contained in the lake to be calculated when combined with an estimate of the area of the lake (1.56 $km^2$ on July 7th 2001) – lake volume in 2001 was thus calculated at 8.0 x $10^6$ $m^3$ (Long, MPhil dissertation), which correlates well with plausible lake volumes given by McMillan and others (2007) for the region. The lake was assumed to be at maximum volume on 7th July in the 2001 melt season, as the lake margins were at the highest levée extents on the western flank and thus any extra discharge into the lake would cause overspill into another basin (Marston, 1983; Long, MPhil dissertation). The elevation profile traversing the lake is given in figure 9 with the data from 2001 illustrated in black. Using the LandSat data from 24th June 2008, a lake profile has been reconstructed (shown in figure 9 in red) that suggests the lake area is just 1.12 $km^2$, with an average depth of 4.6m; thus lake volume on 24th June 2008 is just 5.2 x $10^6$ $m^3$ which is much less than that given for 2001, and correlates well with observed lake extent shrinkage between 2001 and 2008 images. By the second collected image in 2008 (26th July), the lake has almost completely drained, and so it is impossible to tell when the lake reached maximum volume. As Greenlandic supraglacial lakes are

capable of draining in a matter of hours (Das et. al., 2008), the lake discussed above could have been growing in volume until a few hours before the image was collected, before draining through a moulin at its base. Assuming, however, that the lake evolved to its 2001 extent (which is the maximum volume it is capable of reaching) around a similar time to when it reached maximum volume in 2001, the lake would have increased its volume by another c.2.8km x $10^6$ $m^3$ in two weeks. Results from van de Wal and others (2008) suggest that over the past 17 years, the south and eastern margins of the Greenland Ice Sheet have been experiencing increased ablation rates (currently 50% of the ice sheets mass loss is accounted for by ablation and runoff), and thus there is high meltwater availability to fill lakes over short timescales such as the two week filling period discussed above.

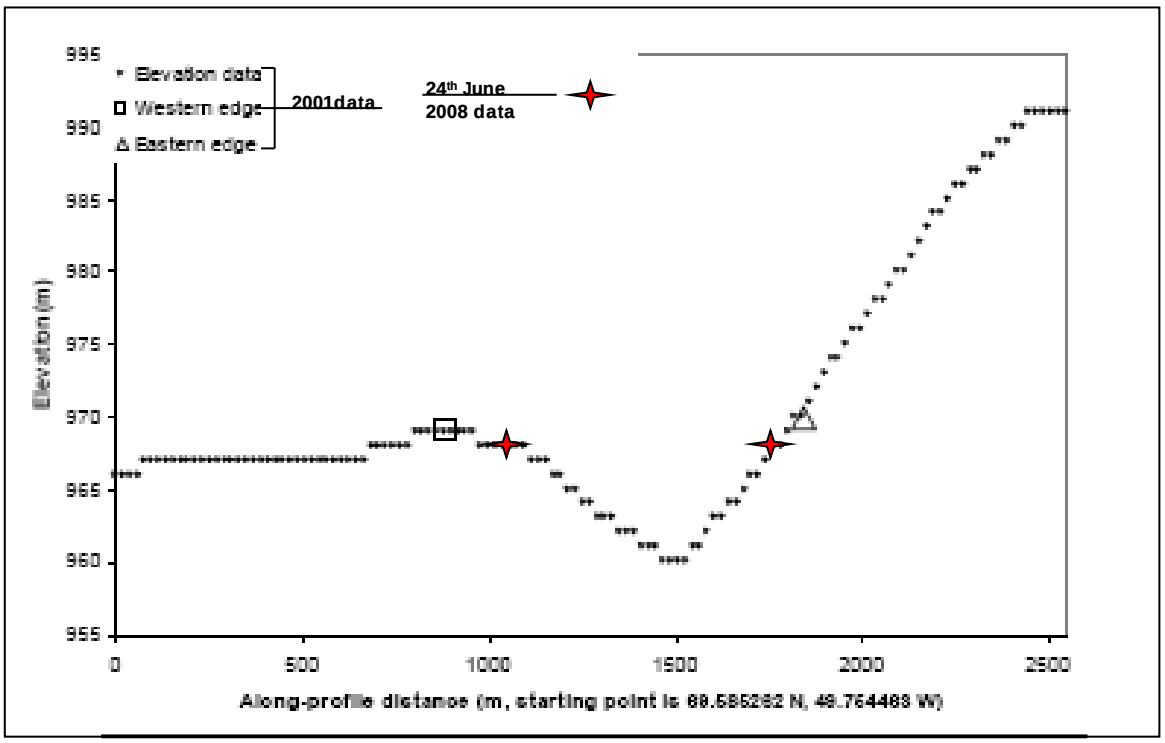


**Figure 9: Elevation profile of the large lake shown in figure 4, derived from flightline traverse over the lake as shown in figure 2. Lake extents are given for 7th July 2001 and 24th June 2008 as shown in the lake margin positions from the respective LandSat images collected for these dates.**

### 3.2. Static analysis

#### 3.2.1. Static DEM hydrological analysis

Upon uploading the available DEM into ArcView GIS software, a static analysis of Paakitsoqs supraglacial hydrology was enabled. By contouring the DEM, figure 10 shows the relatively consistent slope from the inland ice towards to the ice margin.

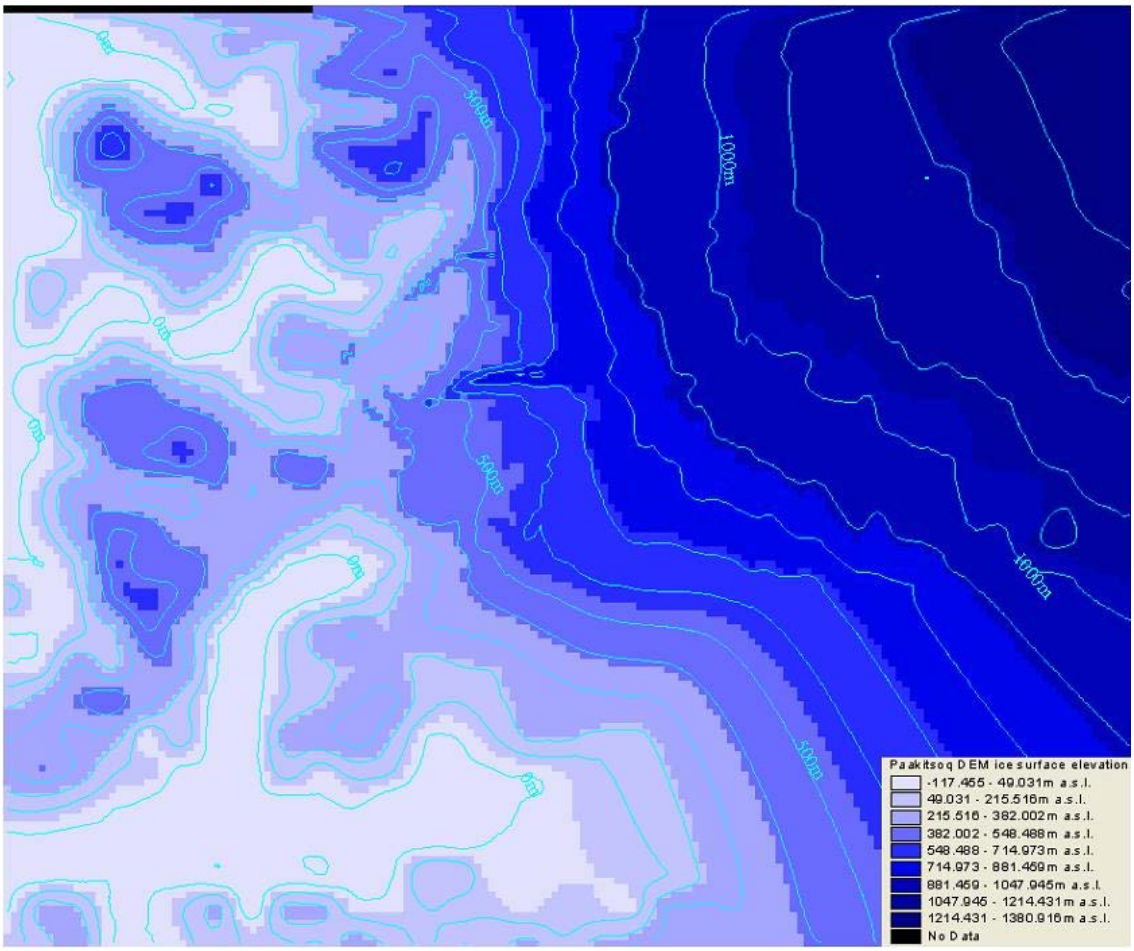


**Figure 10: Surface elevation of the ice sheet and surrounding land-margin at Paakitsoq (contour elevations are meters above sea level; DEM extent is 80.5km by 67km). Ridges over the non-glaciated part of the study area (see figure 5) resulted from data manipulation during DEM kriging and interpolation.**

One tongue of ice, with much steeper slopes, does extend c.7-10km from the ice margin, although this is an anomalous gradient when compared with the uniform gradient of the rest of the DEM surface. When 'sinks' are identified on the DEM (figure 11), they correspond well with observed (or mapped) hydrological features on the ice surface, and the sink closest to the ice margin, associated with the steeply sloping tongue of ice discussed above, corresponds with a channel morphology and crevasse or moulin feature mapped by Thomsen and others (1988), later identified by Long (MPhil dissertation) from 2001 data, and identified again in the present study.

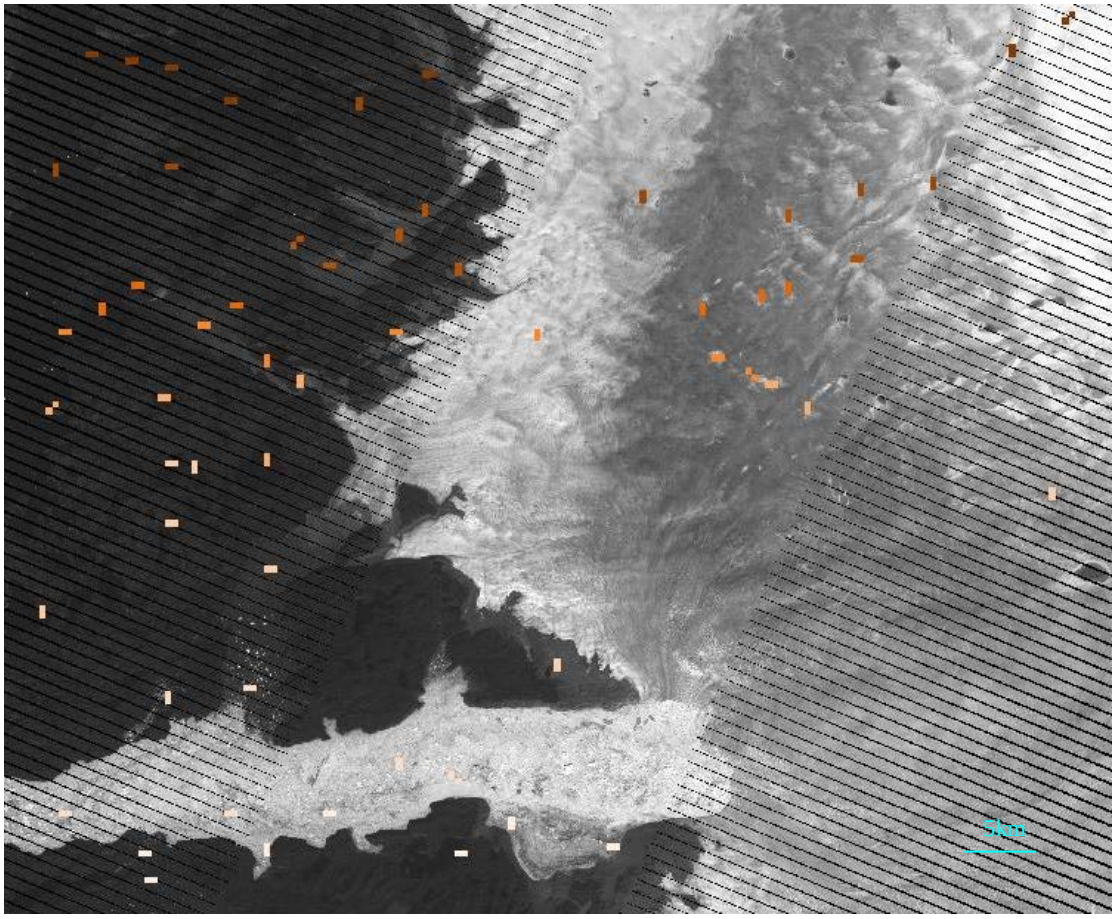


**Figure 11: (coloured) sinks in the DEM surface as visualized using the static supraglacial hydrological routing routine in ArcView 3.3 overlaid onto a collected (11th August 2008) greyscale LandSat image of the study area.**

The remaining sinks are all located within c.600m of visible surface hydrological features in the 24th June 2008 image, which is similar to Long's (MPhil dissertation) value of c.500m between sinks and surface hydrological features identified in a July 2001 satellite image. These features are also mapped by Thomsen and others (1988), either as in-situ lakes, or relict lake basins that manifest themselves as depressions on the ice surface. Large lakes that occur at the greatest distance to the flightlines (used for the creation of the elevation model) are not present as sinks on the DEM, however, as errors in the DEM interpolation process fail to resolve the lake basins. Despite this, the good correlation between modelled sink location and actual or relict lake locations on the inland-ice surface suggests that the DEM is capable of resolving topographic minima (Long, MPhil dissertation), especially those associated with supraglacial lake and channel morphologies, to an extent that allows further analysis via semi-distributed numerical modelling techniques to be applied, and to an extent that will provide accurate modelling results for the Paakitsoq region.

### 3.2.2. Surface drainage network analysis

The supraglacial flow accumulation pathways modelled on the DEM surface correspond reasonably with observed and mapped surface channel features at Paakitsoq. Channels are identified that have a minimum number of upstream feeder cells (in this case on a log scale from 0-100, with no cells being identified as no colour, to 100 cells being identified as the darkest green) and are visualized in ArcView 3.3 software. Errors in the DEM interpolation process cause flow accumulation across non-ice surfaces, whose resulting channels should be ignored. Further, where the DEM expresses uniform slope and interpolation error to the south east of the study area, seemingly laminar flow prevails over the surface of the ice sheet at the accumulation scale chosen – Long (MPhil dissertation) suggests from sensitivity tests that a minimum accumulation of 10 upstream cells provides the highest number of distinct, individually identifiable channels, and this is the case for the areas of the inland ice below the snow line where large lakes form. However, in the south east of the study area, this number of accumulation cells causes widespread flow across a large section of the ice sheet surface, rather than in supraglacial streams and therefore must be ignored as this type of surface meltwater flow is not identifiable in either the available satellite imagery or Thomsen and others (1988) mapped surface hydrological system. It is necessary to use this scale, however, as small surface channels that feed lakes that are identifiable in the 2008 LandSat images are resolved by the surface routing analysis with the minimum number of upstream cells that cause the laminar flow prevalence across the south eastern study margin, and if this scale were changed, these channels would be lost from the surface routing analysis.

The surface drainage network modelled in ArcView 3.3 is shown in figure 12, below. Dark green channels are the streams that receive most water from their feeder cells. Regional topographic variations influence the morphology of surface meltwater flow accumulation pathways and cause supraglacial streams to run off the ice surface to the ice margin – it is here where extensive networks of supraglacial channels are visualized, but in reality, satellite images and mapped (1988) features do not correspond with the modelled output.

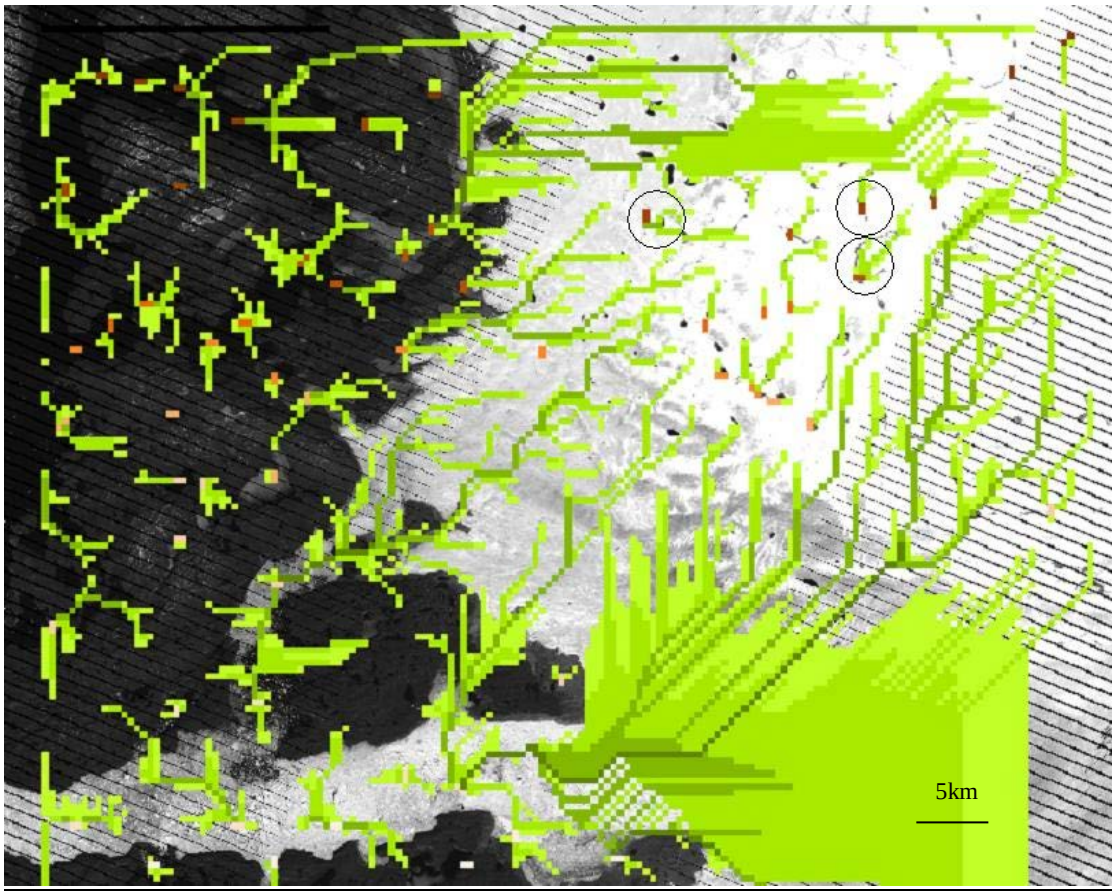


**Figure 12: Supraglacial flow accumulation network as identified by the surface flow routing analysis in ArcView 3.3. Accumulation pathways are shown in green, with lighter colours indicating fewer upstream feeder cells than darker colours. Sinks are also identified in the image (shown as orange rectangles) and it is clear that in the central Paakitsoq region, surface drainage channels feed these sinks, and these individual channels (and surface lakes formed in the sinks) are often identifiable in the 2008 LandSat images. The three circled sinks and accumulation flow pathways leading into the sinks are discussed further in the text below.**

The mapped supraglacial channels from 1988 are moulin-terminating (Thomsen et. al., 1988), rather than running off to the ice margin, while the presence of small lakes at the ice marginal region does not correspond well with extensive surface channel formation (as this implies widespread dynamic hydrological activity rather than limited surface run off into smaller lakes). The lack of supraglacial channels running off the ice sheet surface in the 2008 satellite images suggest that most melt water that doesn't refreeze flows into surface lakes (and moulins) rather than running off the ice sheet as the modelled accumulation pathways suggest. This is similar to the findings of Thomsen and Braithwaite (1987) in their investigations into the use of remote sensing to determine run-off regimes at the margins of the Greenland Ice Sheet. Local

variations in elevation extent (namely depressions in the ice surface) cause accumulation flow pathways to terminate in modelled sink locations (corresponding to surface lakes). Three sinks and accumulation flow pathways leading into the sinks are highlighted in figure 12 (circled), as these sinks correspond to lakes identified in the 24th June and 26th July 2008 LandSat images and because the flow accumulation pathways match supraglacial channel formations in the satellite images collected. Figure 13 shows these three sinks and flow accumulation pathways in more detail, and illustrates the correspondence between modelled sinks and surface drainage channels, and observed features (from the 24th June 2008 LandSat image).

Inland from the ice margin, modelled accumulation pathways correspond well with observed features (both mapped and identified in 2008 LandSat imagery), but as distance from the ice margin decreases, this good correlation of observed and modelled features begins to decrease. This is also suggested by Long (MPhil dissertation) who proposed that there is a shift between supraglacial routing regimes in the inland ice and the marginal regions as visualized in ArcView 3.3. Ice marginal drainage is dominated by moulins, and small lakes fed by small surface drainage channels. These features are unable to be resolved at the scale of the DEM and cause modelled accumulation channels to simply run off the ice surface. Inland ice drainage, however, is dominated by large lake formation with larger supraglacial drainage

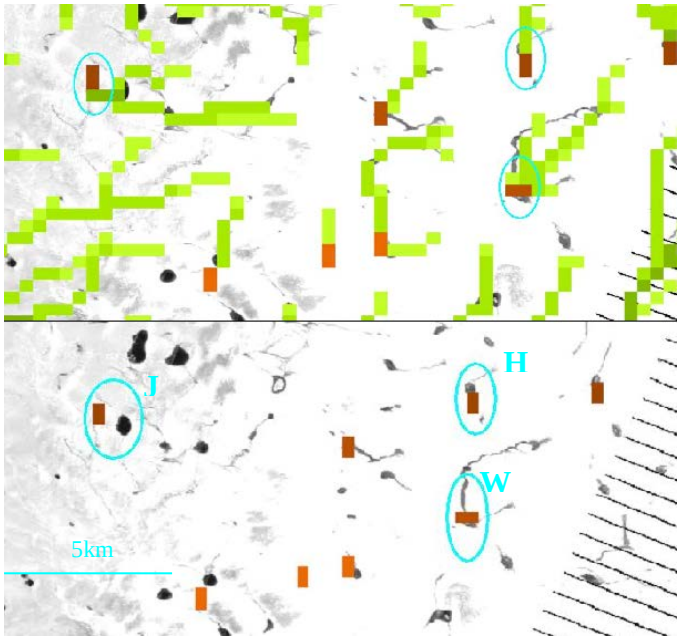


**Figure 13: Detail of three sinks and accumulation pathways (circled) that are identified as being lakes with surface channels in the June 2008 satellite image. The top image shows modelled surface drainage routes, while the bottom image shows the sinks as lakes with filled or relict channels feeding them that correspond well to the modelled drainage routes. These sinks exhibit lakes within c.400m of their modelled position in the June and July 2008 LandSat images, although the lakes have all drained in the August 2008 image.**

channels and morphologies, which can be resolved (if coarsely) by the DEM and with a good correlation between their modelled and actual locations.

### 3.3. Static volumetric analysis of supraglacial lakes

The three lakes presented in figure 13 were subject to analysis in ERDAS Imagine 9.0 GIS software and calculations of their respective areas were made based on the available June and July LandSat imagery. It is known that the darkest section of lakes identified in satellite imagery is correlated with the maximum lake depth profile (due to the absorption of optical wavelengths – Sneed and Hamilton, 2007), and with observed lake depths measurements from other research studies, average lake depth estimates were made for Lakes *H*, *J* and *W* in order that lake volume can be estimated.

The mean lake depth observed by McMillan and others (2007) at Swiss Camp at the beginning of July 2001 was 1.5m ± 0.7m, while Echelmeyer and others (1991) identified surficial lakes with depths of as little as 10cm to over 20m in the Paakitsoq region north of the Jakobshavn Isbrae. From these data, estimates about the depth of the three lakes in both satellite images were made (for the dates of 26$^{th}$ June and 24$^{th}$ July). In the June image, lake *J* was assumed to be no less than twice as deep as the other two lakes due to it being a much darker shade of blue than the lakes *H* and *W*, and it's correlation in colour to the larger lake above it (for which depth data is previously known in 2001 – after Long, MPhil dissertation) suggests its average depth is c.4m. Thus lake *H* and lake *W*, with similarly coloured extents in June 2008 are estimated to have an average depth of c.2m at the time of the satellite image collection. By the July 2008 image, however, these depth estimates have to be revised as lake drainage, or filling is in process – lake *J* is much lighter than previously, and has shrunk in area a great deal compared to the June image. This shrinking area suggests that average lake depth is similarly reduced (as the lake basins are constrained by topographic minima, and a reduction in area will be accompanied by a reduction in lake depth), and an estimate of average lake depth in the July image is c.0.8m (similar to McMillan and others (2007) observations for the same date). Lake *H* also decreased in area between June and July as observed in the LandSat images, and an estimate of its average depth in the July image based on its lighter colouration than lake *J* is c.0.4m. Lake *W*, however, grew substantially in area between the June and July image collection and its colouration deepened (though not quite as much as lake *J* in the June image) – as a result the average depth estimate for lake *W* by the collection of the LandSat image in July is c.3m. These estimated average depths and

the observed supraglacial lake areas were used to calculate an estimated lake volume for each of the three lakes at the dates of the LandSat image collection. Table 1 shows the measured areas, estimated depths and estimated volumes of lakes *H*, *J*, and *W* for the 24th June and 26th July as calculated from the satellite imagery:

| Lake/Date | Elevation | Observed area (km2) | | Estimated average depth (m) | | Estimated volume (m3) | |
|---|---|---|---|---|---|---|---|
| | | 24th June | 26th July | 24th June | 26th July | 24th June | 26th July |
| H | 1146m a.s.l. | 0.249 | 0.056 | 4.0 | 0.8 | $1.90 \times 10^6$ | $0.07 \times 10^6$ |
| J | 937m a.s.l. | 0.467 | 0.084 | 2.0 | 0.4 | $0.50 \times 10^6$ | $0.22 \times 10^6$ |
| W | 1100m a.s.l. | 0.294 | 0.499 | 2.0 | 3.0 | $0.60 \times 10^6$ | $1.50 \times 10^6$ |

**Table 1: Vital statistics of three supraglacial lakes identified on the surface of the Greenland Ice Sheet at Paakitsoq, where observed lakes match the position of modelled sinks on the DEM surface. Lakes H and J drain partially between the June and July LandSat images collected, while lake W increases its volume. All lakes drain by the collection of the August (11th) 2008 LandSat image.**

Although lake *W* appears to fill between June and July (compared to the draining of lakes *H* and *J*), this may not represent the actual volume of water produced on the surface of the ice sheet at Paakitsoq, as the moulin at the base of lake *W* may drain water from the lake (at a rate less than the observed filling) – and thus if the lake were totally ice dammed the volume may be larger than that estimated for the 26th July. However, for the purposes of the present study, it is assumed that the lake remains ice dammed until the 26th July 2008 and this may well be the case considering the lakes increase in volume through the melt season and the fact that it is located at 1100m elevation – previous studies suggest filling lakes at similar elevations may remain ice dammed at this time in the ablation season and thus their observed lake extents and estimated volumes are a true representation of their vital statistics at the time of the satellite image collection (McMillan et. al., 2007).

The start of the melt season at Swiss Camp in 2007 was identified by Painter and others (2007) as beginning on the 5th May and according to the authors, this is also likely to represent the date of the beginning of the melt season at similar elevations to the north and south of Swiss Camp and at similar times every year. Swiss Camp is located at 1170m elevation, similar to the elevation of lake *H*, and at a higher elevation than both lake *W* and lake *J*. As a result, it is assumed that the beginning of the melt season occurs earlier at lower elevations (after Painter et. al., 2007; McMillan et. al., 2007), and thus filling of lake *J* begins 8 days earlier than the filling of lake *W* (beginning to fill on the 3rd May), with the higher elevation lake *H*

beginning to fill on 5th May 2008. This early filling of lakes at lower elevations is visible in the collected satellite images in 2008, as discussed above.

Using the data given in Table 1, a graph was produced to represent the inception and evolution of supraglacial lakes *H*, *J*, and *W* volumes over the course of the 2008 melt season. This graph is given in figure 14:

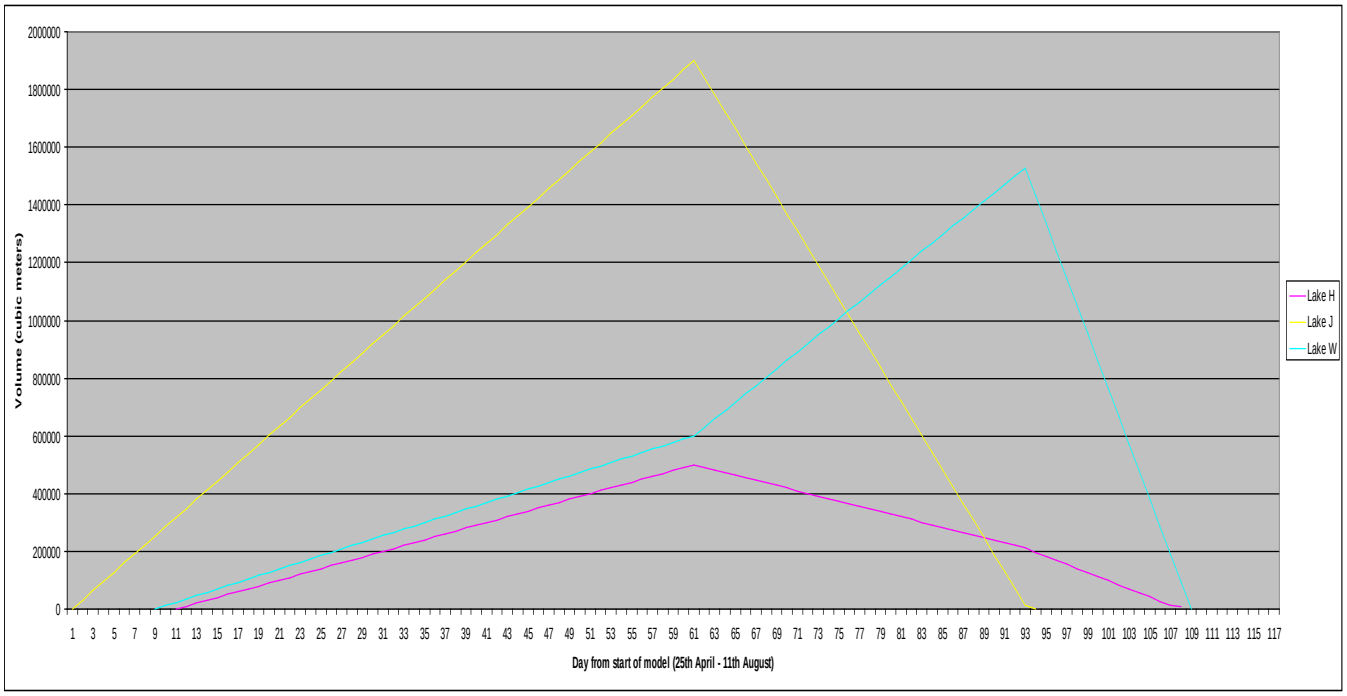


**Figure 14: Estimated surface lake volumetric evolution based on observed lake measurements, estimated lake depths, observed start of melt season date and assuming a constant filling/draining rate per day between the start of the melt season at Paakitsoq and the collection of the August 11th LandSat image where all three lakes had drained.**

Lake *J* fills to its greatest extent by the 26th June, and drains completely by July 24th. Lake *H* fills at a much slower rate to lake *J*, begins to drain after 26th June, and drains at a faster rate after 24th July. Lake *W* fills at a similar rate to lake *J* until the 26th June when the filling rate doubles until the 24th July. It drains rapidly and completely by the 11th August.

### 3.4. Modelling supraglacial lake evolution at Paakitsoq

*Lake watersheds*

Watersheds were produced for lakes *H*, *J* and *W*. A detailed description of the methods behind the watershed creation is given in Appendix A, and the watersheds are shown in figure 1C overlaid on the DEM of the region. These watersheds are computed within the numerical model, and their details as derived from ArcView 3.3 software are given in table 2 below:

| Lake watershed | Number of DEM cells | Area ($km^2$) |
|---|---|---|
| H | 65.5 | 16.4 |
| J | 19 | 4.8 |
| W | 141.9 | 35.5 |

**Table 2: Watershed details of the areas draining into each of the three lakes discussed above.**

The watersheds shown in table 2 are used in the numerical model to determine the delay in routing of surface meltwater between the cell of meltwater creation and the pour point (sink) on the DEM.

### 3.4.1. Initial test

The model was run initially for 50 days starting in the late melt season in 2007 – from 1st September. The modelled discharge at an arbitrary pour point (moulin) at an elevation of 930m above sea level is given below in figure 15, and the model output is given as cubic meters per second. The modelled area was not overlain by a snowpack.

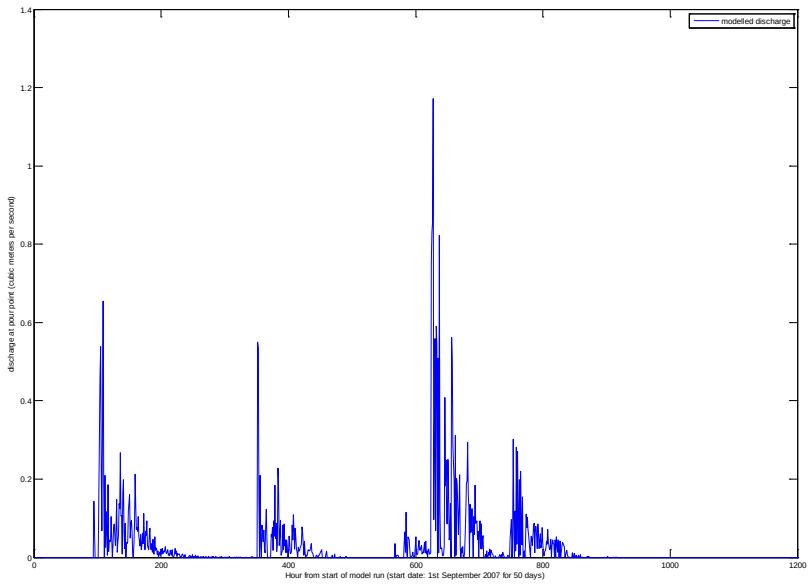


**Figure 15: Trial run of the combined energy balance and surface routing models for an area of the Paakitsoq region (as defined in the previous sections of the present study), with modelled discharge at a pour point identified in the DEM surface for the end of the melt season in 2007. Initial model results suggest that a substantial amount of modelled melt water does not enter the pour point.**

As can be seen in figure 15, the model deals with surface melting and subsequent routing of this meltwater to a location on the DEM surface (a pour point, or ice-dammed moulin that will cause a surface lake to develop), and the data outputs are able to resolve both diurnal fluctuations in meltwater production and longer-scale

fluctuations in discharge. The diurnal fluctuations are visible as a 'saw-toothed' pattern within the graph, and fluctuate with a periodicity of around 12 hours. The longer-scale variations are expressed in four periods of steeply rising discharge returns, followed by a subsiding rate of discharge. These longer periods of varying discharge last around 100 hours, with typical peak discharges within 10 hours of the start of the rising limb. Secondary peaks of rising discharge occur within 36 hours of the initial, strongest peak of discharge.

By multiplying the given output by 3600 (the number of seconds in an hour), an hourly discharge, and therefore hourly volume of meltwater being routed to the identified moulin can be calculated and these data can be compared to observed lake volumes derived from the satellite images collected in 2008 – this is done for the three lakes identified in the static lake analysis and LandSat images discussed above (lakes *H*, *J* and *W*) and the data is given and discussed below.

### 3.4.2. Modelled volume of lake *H*

The model was run for 128 days (until the data are too recent to be collected from the AWS and therefore unavailable from the Steffen Research Group) starting on the estimated date of the beginning of the melt season (Julian day 125) at the elevation of lake *H* (1146m above sea level). The model output is given below in figure 16 and represents the modelled discharge theoretically passing through the sink identified as representing the moulin at the base of the observed lake *H*. If the moulin is ice-dammed, the lake will fill at a rate equal to the discharge into it, and thus a rate of filling (and volumetric increase) can be accounted for – and compared to observed volumetric changes as discussed above.

**Figure 16: Modelled discharge delivered to the pour point at lake *H*.**

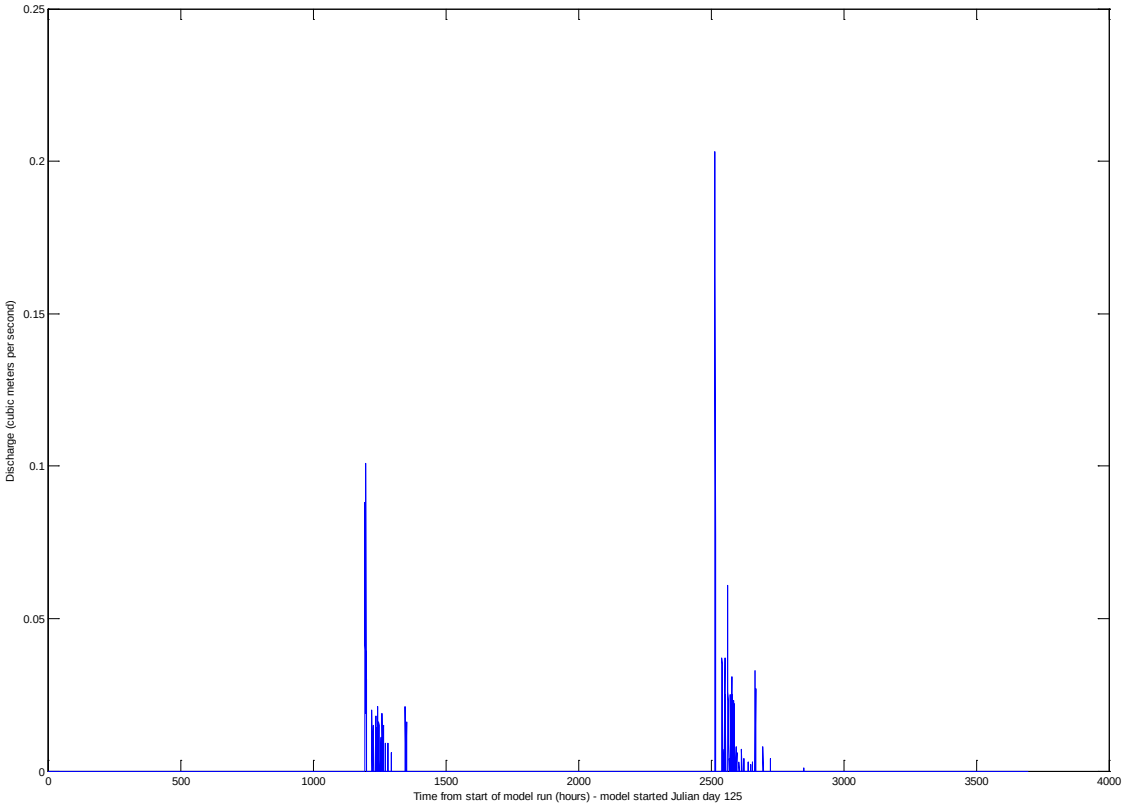


The results indicate two distinct occasions of filling of the lake, between Julian days 149-155 and between Julian days 205-212, that are separated by extended periods with no meltwater production (of over 1150 model hours each). The first of these blocks of filling experienced a maximum discharge of 0.1 cumecs (cubic meters per second) with an average filling rate of below 0.02 cumecs, whereas the second filling period experienced more prolonged and greater filling rates, with a maximum discharge of 0.2 cumecs and an average filling rate of 0.25 cumecs. There is evidence of diurnal fluctuation in discharge into the pour point, but this is limited compared to the diurnal pattern modelled in the initial test run.

When these data are transferred into volumes of water, the volumetric evolution of lake *H* can be estimated. From the modelled discharge results, the lake will attain a volume of 2019.6m$^3$ by Julian day 177 (the date of the collection of the June LandSat image), increasing to 5571.1m$^3$ by Julian day 205 (the date of the July LandSat image collection). Unlike the model results, by assuming a constant filling rate between these dates (as meltwater is likely produced each day during the ablation season – Zwally et. al., 2007), the volumetric evolution of lake H throughout the melt

season (as calculated by the model) can be plotted, that will then correspond with the graphic estimate of observed lake evolution as produced from the LandSat images above. Figure 17 shows the modelled volume of lake *H*, throughout the melt season in 2008, assuming it does not undergo drainage (which the model cannot account for):

**Figure 17: Lake *H* modelled volume**

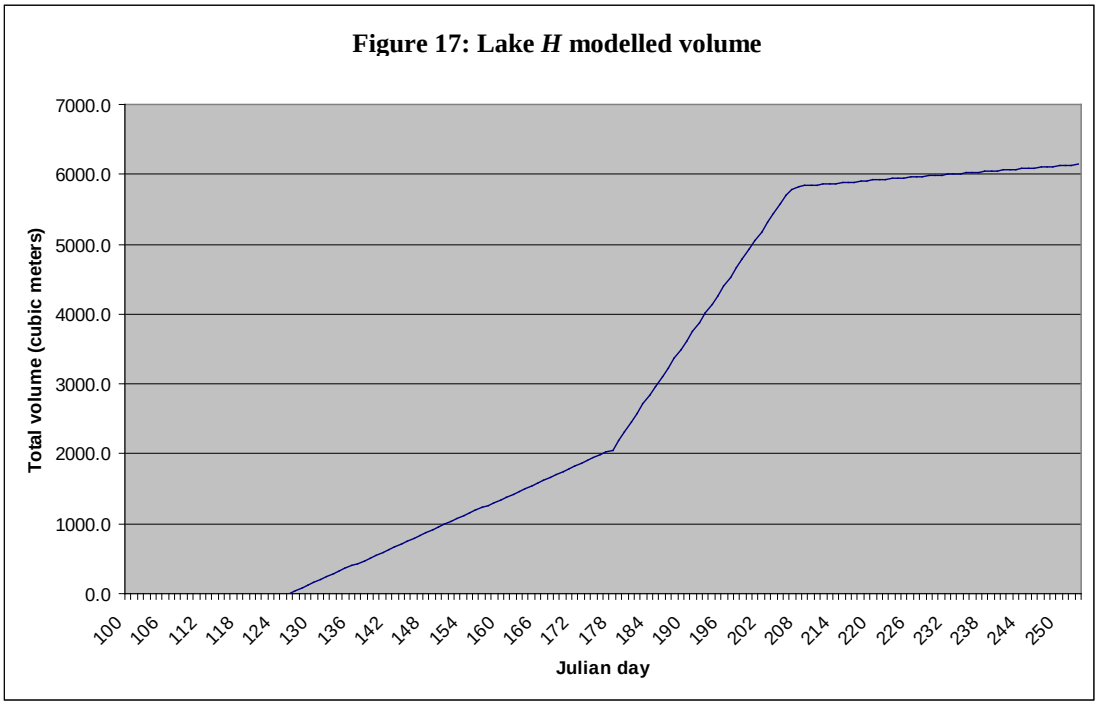


Three phases of filling are suggested, with a slower rate of filling until June 24th, a tripled rate of filling between 24th June and 26th July, and a much slower rate of filling until the end of the dataset available to run the model. The lake reaches its maximum volume of 6138m$^3$ at the end of the model run (11th September). This rate of filling and maximum volume is compared to the estimate of observed lake volume evolution for lake *H* in figure 18, and the graph suggests substantial differences between the observed lake volume and the modelled volume.

Figure 18 suggests that the total modelled volume of Lake *H* is over 81 times less than the estimated observed maximum lake volume (as observed on 24th June 2008). The lake starts draining after this point, and therefore the total volume of water that lake *H* has actually 'consumed' is far greater than this, and so the difference between observed and modelled melt water production is also much greater. Further, the model suggests that the maximum rate of filling of the lake occurs after the lake has been observed to start draining, and thus it is impossible in the present study to determine whether in reality the filling rate of the lake was also at its highest around this date (as the filling rate may have increased, but not enough to counter-act the

draining rate of the lake once the ice damming of the moulin draining the lake basin had begun to melt). However, a vast amount of meltwater produced in the model does not reach the pour point (more than $10x10^7$ $m^3$) and if this did, modelled lake volume at the date of observed maximum volume would be 10 times greater than the actual estimated volume.

**Figure 18: Lake *H* modelled vs observed volume**

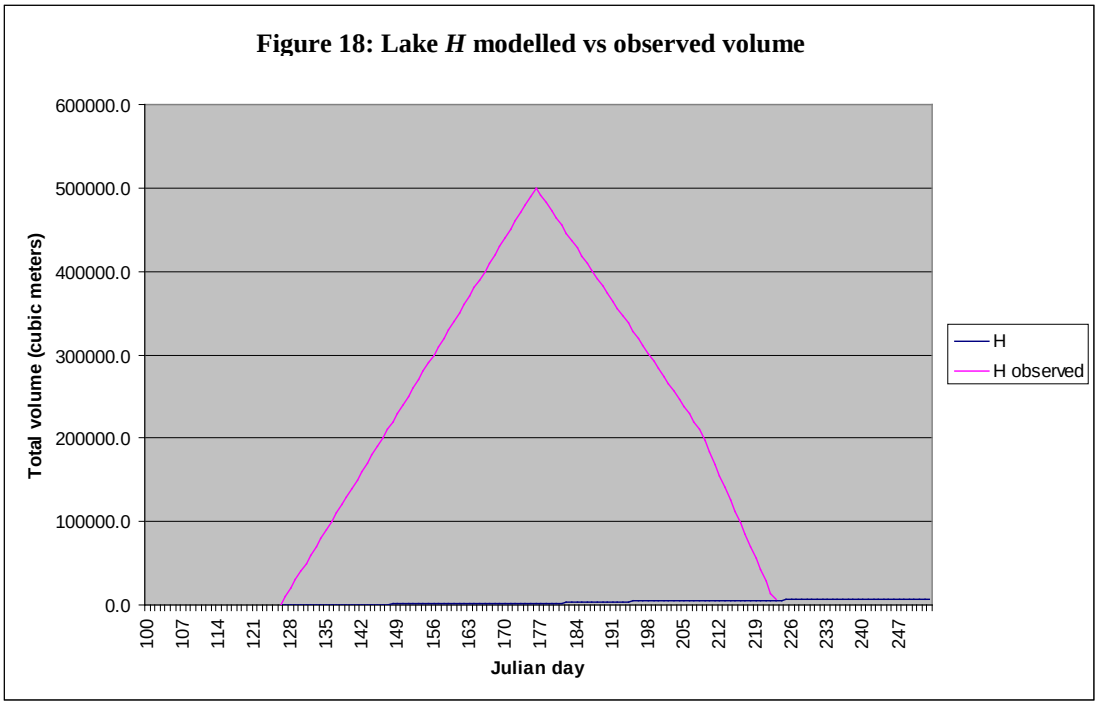


### 3.4.3. Modelled volume of lake *J*

As for lake H, the model was run from the predicted beginning of the melt season for the elevation of lake J (937m), starting on Julian day 115 and running for 138 days until MET data are unavailable. Figure 19 represents the modelled hydrograph for the moulin at the base of lake H throughout the ablation season.

Model results suggest three peaks in the hydrograph filling lake *J*, with filling periods lasting between 100-230 hours and lengthy periods separating these filling times that last around 1000 hours. Maximum discharge was attained in the first period of lake filling, 1200 hours into the model run (on Julian day 149) and peaked at 1.38 cumecs (equating to $4932m^3$ of modelled water entering the lake in an hour). The second stage of filling of lake *J* attained only a maximum discharge of 0.8 cumecs (Julian day 204), and averaged around 0.1 cumecs for a period of 5 days (compared to the first filling event which averaged 0.16 cumecs for a period of 8 days). The third

stage of modelled filling occurred much later in the melt season (Julian day 254 – 2nd September) and was characterised by a 4 day period of low discharges (peaking at 0.1 cumecs and averaging 0.04 cumecs). Diurnal fluctuations in filling are less clear than in the model results for lake *H*.

**Figure 19: Modelled discharge delivered to the moulin at the base of lake J.**

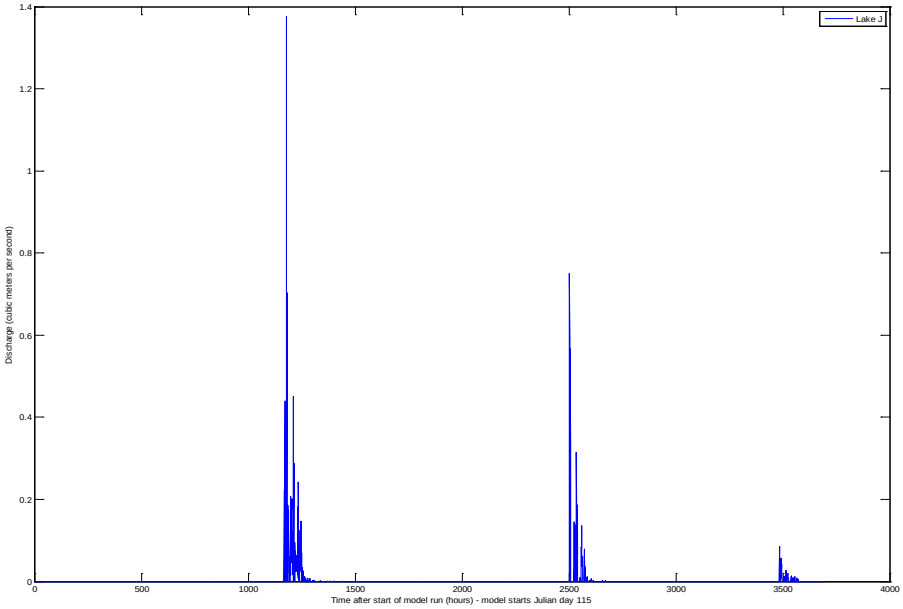


Manipulating the data into volumes, lake *J* will attain a volume of over 32000m$^3$ by the June LandSat image collection date and reach a volume of over 47300m$^3$ by the collection date of the July image. The lake continues to fill until the data are unavailable, evolving to a maximum volume of 50896.8m$^3$ by the end of the model run. This data is presented in figure 20 below (and assumes constant filling rates to account for the comparison between estimated observed lake volumes and modelled lake volumes at the dates of the LandSat collection, as discussed previously). Two main phases of filling are suggested – a period of high filling rates before July 26th and a period of much slower filling after this date (although there is a slight decrease in the filling rate between June 24th and July 26th). At its fastest rate of filling, lake *J* is modelled to fill at a rate of 1000m$^3$ every 18 days. However, this modelled filling rate is much less than the estimated observed filling rate of lake *J* (that is estimated to fill at 20000m$^3$ every 5 days between the beginning of the melt season and the 24th June, and this difference is illustrated in figure 21.

**Figure 20: Lake *J* modelled volume**

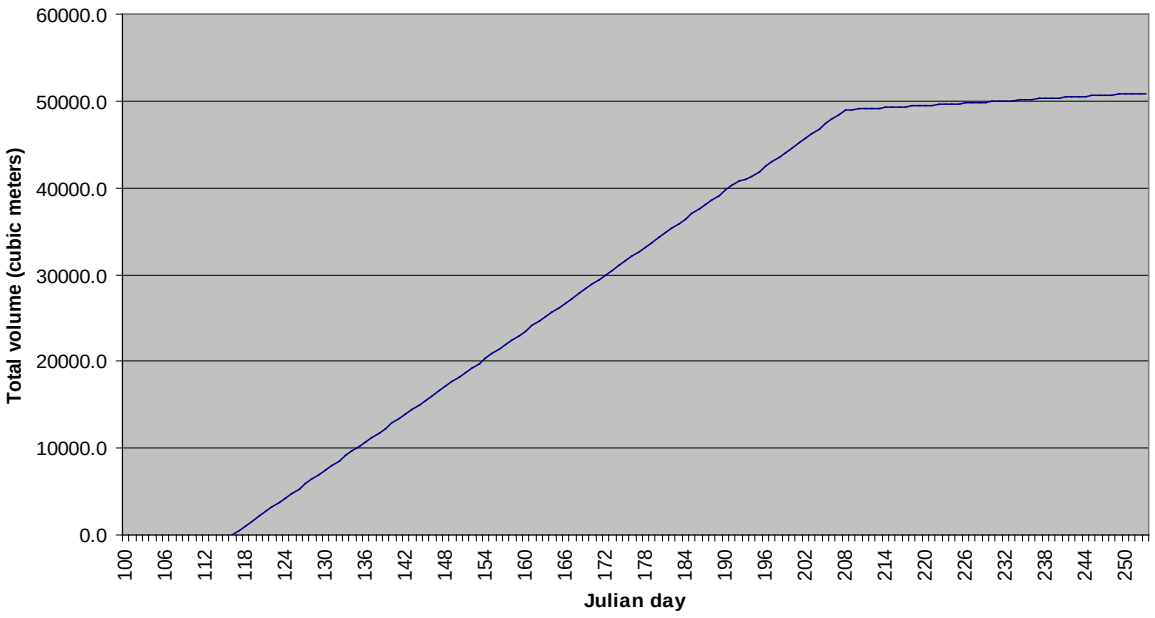


**Figure 21: Lake *J* modelled vs observed volume**

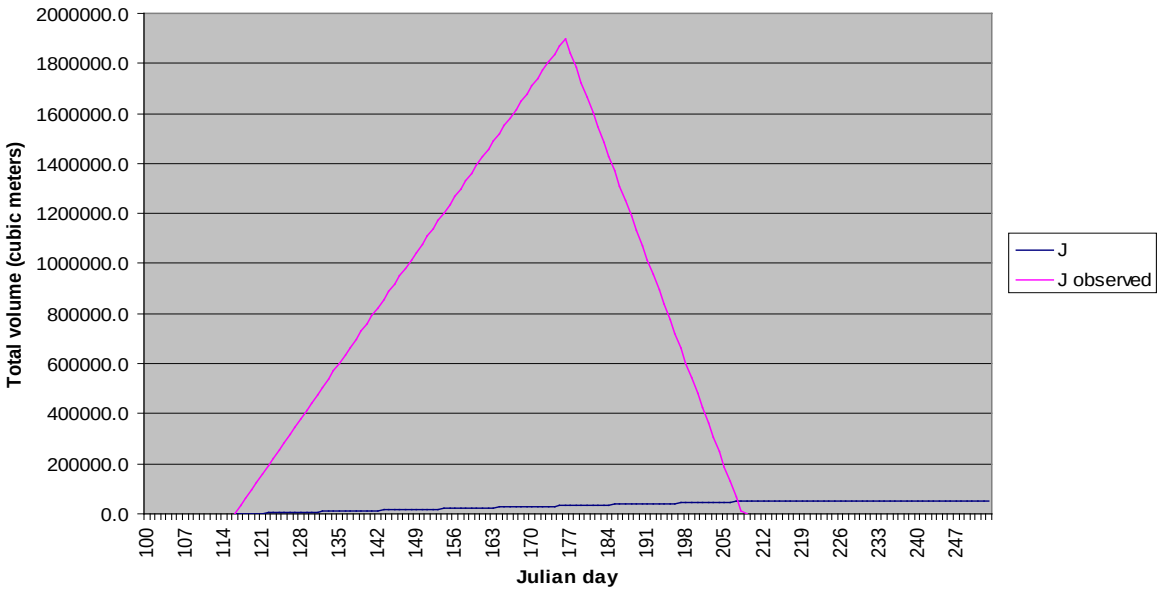


Again, a large volume of meltwater is produced in the model, but not routed to the moulin. This lost meltwater exceeds $30x10^7$ $m^3$ in total, and accounts for over 95% of the meltwater produced within the model – had this meltwater been routed to the moulin, the volume of the modelled lake at the date of the observed maximum volume would have been over 40 times greater than the actual estimated volume (around $78x10^6$ $m^3$ compared to $1.8x10^6$ $m^3$).

### 3.4.4. Modelled volume of lake W

The model was run for 130 days from Julian day 123, the start of the melt season for the elevation of lake *W* (1100m). Figure 22 shows the model output hydrograph for the discharge into the moulin at the base of the lake:

**Figure 22: Modelled discharge at the pour point in lake *W*.**

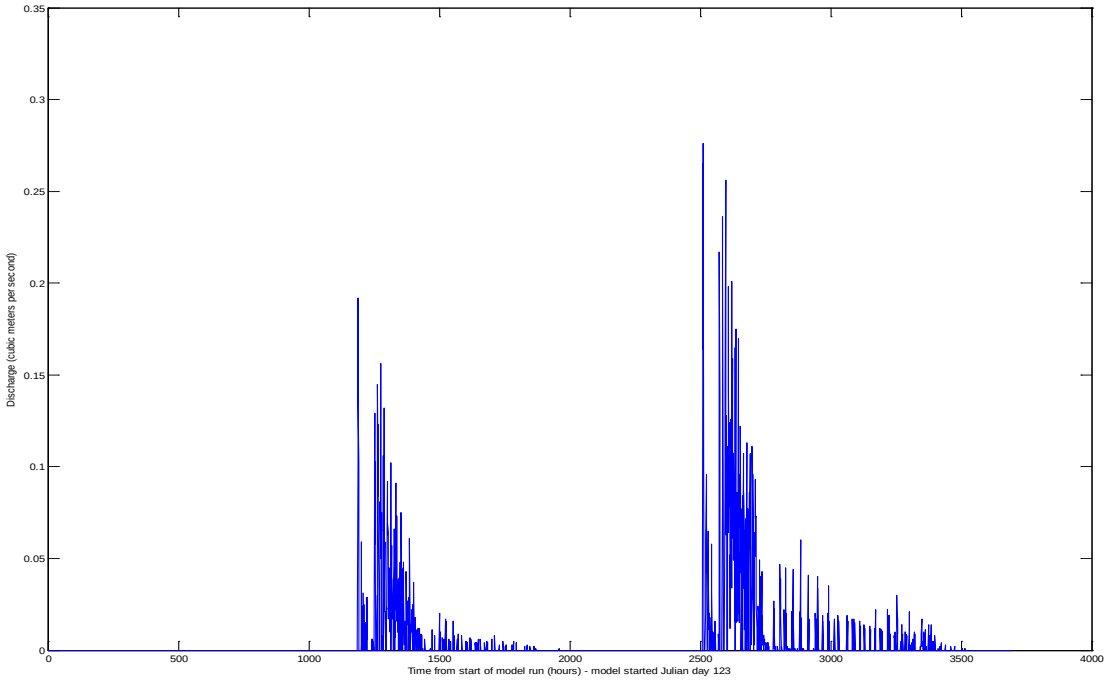


The returned hydrograph exhibits strong diurnal fluctuation especially in the falling limb of the two identifiable periods of discharge into the moulin. These periods of discharge are extended over 750 hours and 1000 hours respectively, with the first period being shorter than the second. The first period of discharge peaks at 0.18 cumecs initially, and then experiences a second lower peak of 0.16 cumecs 3 days later, with an extended falling limb of discharge over the next 200 hours, decreasing to a diurnally fluctuating period of 0.02 cumecs for the next 17 days. The second period of discharge lasts over 40 days, and experiences a very sharp peak of nearly 0.26 cumecs on the 27$^{th}$ July, followed 4 days later by a further peak of over 2.4 cumecs and an extended period of discharge averaging over 0.1 cumecs for 4 days. After this, a falling limb of diurnally varying discharge fluctuating between 0.03 cumecs is modelled for a period of 700 hours until the 3$^{rd}$ September.

When the discharge data are transferred into volumes and the data are plotted on a graph of constant filling rates, the modelled output suggest that the lake fills at an ever increasing rate throughout the ablation season as shown in figure 23:

**Figure 23: Lake *W* modelled volume**

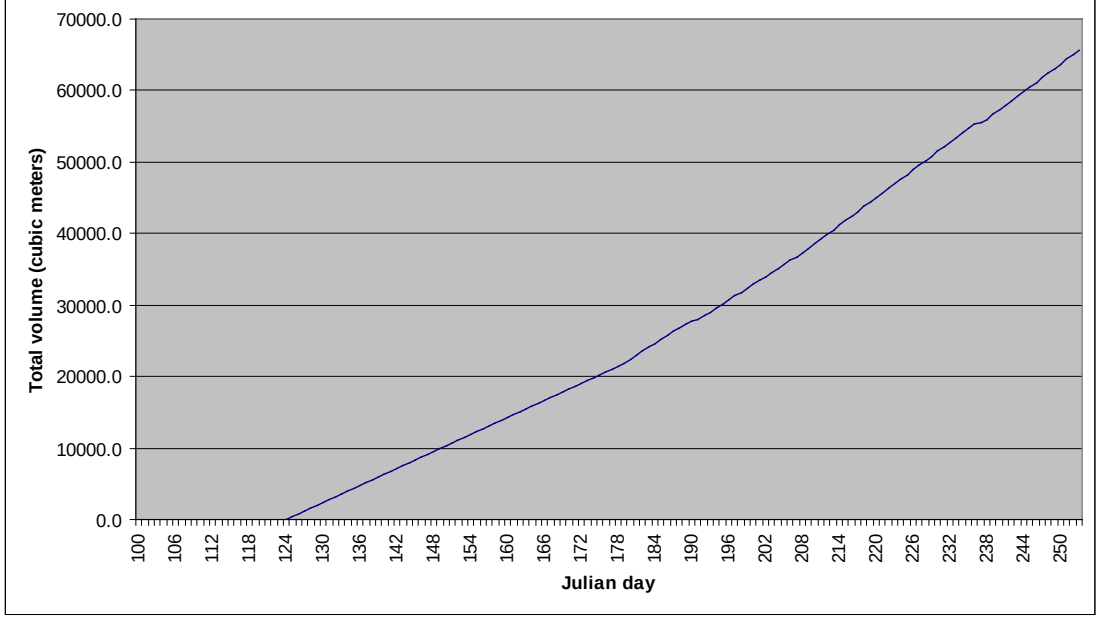


The maximum volume of the lake is 65642.4m$^3$ by the end of the model run. This is considerably less than the maximum estimated observed volume of over 1500000m$^3$ occurring on the 26$^{th}$ July. At this date, the volume of the modelled lake is 40 times les than this at just under 37300m$^3$, while previously on the 24$^{th}$ June, the modelled lake volume (20571m$^3$) is 30 times less than the estimated observed volume (600000m$^3$). Although the modelled lake evolution results suggest that the model deals well with lake *W* filling at a steadily greater extent throughout the melt season (as shown by the increase in observed lake volume between the beginning of the melt season and the June and July LandSat images), it still does not adequately model this increase in filling at a greater rate between the June and July images as shown in figure 24 below. As with the previous model runs, a large quantity of modelled meltwater was not routed to the pour point, and thus a high volume of water was not added to the overall volume of lake *W*. The total volume of water produced by the model, but not routed to the pour point was over 28x10$^7$ m$^3$ which suggests that had this total volume of water been routed to the pour point effectively after it had been produced, the modelled lake volume on the 26$^{th}$ July (when the observed lake reached

its maximum estimated volume) would have been around $17.9x10^7$ $m^3$, compared to just $1.5x10^6$ $m^3$ of water estimated from the LandSat image observation.

**Figure 24: Lake *W* modelled vs observed volume**

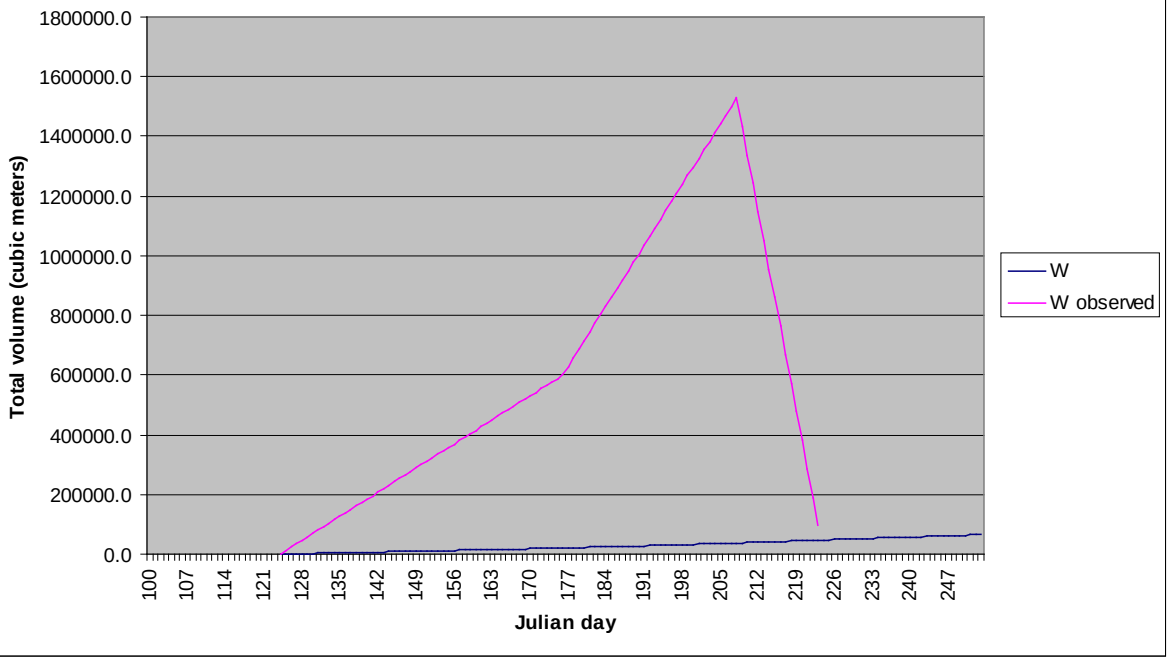


# 4. Discussion

## 4.1. Observed supraglacial hydrological systems

### 4.1.1. Ice marginal surface lake inception, evolution and drainage

The surface hydrological system at the ice margin of Paakitsoq is differentiated from the inland ice system by the apparent lack of surface meltwater throughout all satellite images collected in 2008 compared to that of the inland ice surface. There are a limited number of small lakes, with very few within 1km of the ice margin; there are also a small number of diminutive surface drainage channels, and these channels exhibit underdeveloped morphologies compared to the inland ice surface. Moulin-like features are identified without lake cover – these are also identified in Thomsen and others map (1988) and also in the LandSat images collected in 2008. These features are irresolvable on the scale of the DEM, although it is clear from the satellite imagery that most surface meltwater does not collect in supraglacial lakes, but exits the surface hydrological system by draining straight into the bare moulins, or running off the ice surface at the margin.

Higher mean annual temperatures are predicted at lower latitudes and elevations in the future, as a result of climate warming, and this is likely to increase the duration and the intensity of the ablation season at Paakitsoq (McMillan et. al., 2007), especially in the ice marginal regions. Climate warming is therefore likely to increase the amount of surface meltwater produced on the ice surface, and available to be routed across the ice into topographic minima and create lakes. However, the limited presence of supraglacial lake development on the ice surface in these marginal regions, and subsequent lack of evolution between the June, July and August LandSat images collected in 2008 suggests that an increase in surface meltwater production and availability is unlikely to influence lake inception and drainage in the marginal regions as the water is likely to simply drain into non-ice-dammed moulins. The lack of a well developed supraglacial channel system suggests that ice-marginal drainage does not dominate in this region. This defies Krabill and others (2004) assertions that excess runoff since 1998 (due to climate warming) has affected ice marginal hydrology in coastal ice sheet regions, such as the margins around the Jakobshavn Isbrae (to the south of the present study region), as it is not possible to see the effects of excess runoff on the ice sheet surface in the collected satellite images.

### 4.1.2. Implications of ice marginal supraglacial drainage system structure on ice sheet dynamics and ice marginal hydrology

Research by Zwally and others (2002) showed that surface melt induced speed-up of ice sheet flow north of the present study area (at Swiss Camp) is possible as meltwater propagates to the bed of the ice sheet and through enhanced basal lubrication, allows the imposition of fast ice flow upon normal slow-flow conditions (of ice that is land terminating without outlet glaciers). At Paakitsoq, the marginal regions of the ice sheet to the north of the Jakobshavn Isbrae glacier are likely to exhibit similar flow traits to those investigated and proposed by Zwally and others (2002), as surface meltwater drains straight into moulins throughout the melt season, rather than forming large supraglacial lakes. Closer to the outlet glacier, however, flow regimes will be altered to accommodate the large flux of ice across the glaciers grounding lines (Stober and Hepperle, 2006), and it is hard to propose where the effects of the glacier on ice sheet flow end (as this requires specific investigation through feature tracking

to determine the flow regime around the glacier basin). Further, the limited number of small supraglacial lakes are unlikely to exert much influence on ice sheet flow upon their draining (as that described by Das et. al., 2008, for example), as the volumes of water involved are much smaller than for the larger lakes identified in the satellite images in 2008 at high elevations on the inland ice. However, regardless of the implications for ice flow, the marginal surface drainage system in the region may provide an adequate source of continuous meltwater production (exiting the supra-, en- and subglacial hydrological system at the ice margin in the form of a large proglacial lake) throughout the summer melt season (through rapid moulin drainage) and thus is likely to be the site for a large hydropower energy facility being investigated by the Greenlandic Government (Thomsen and Olesen, 1989).

### 4.1.3. Inland ice supraglacial lake inception, evolution and drainage

The observations from the satellite imagery and static volumetric analysis imply that the ablation period affecting lake volumes (before the lakes drain and surface melt water produced during the later part of the melt season drains straight into moulins) is limited to between 90 and 120 days (from the start of the melt season) and influenced predominantly by the lake basins ice surface elevation. Inland ice lakes (those lakes located at least 10km from the ice margin) closer to the ice margin at lower elevations fill earlier than those at higher elevations because their catchments are exposed to increased insolation receipts earlier in the ablation season. The initial presence of a snow cover often causes lakes to begin filling slowly (as the snow cover causes a delaying effect on surface meltwater routing to the lake basin), but when the snowpack melts and bare ice is exposed, melt rates increase and lakes fill more rapidly (as bare ice has a lower albedo than snow and surface melting increases). Lake drainage depends on a number of factors that influence the ice fracture mechanics (Van der Veen, 1998) that allow the ice dammed moulin to crack open and drain the lake and although the present study does not concern lake drainage explicitly (as the numerical model used does not deal with lake drainage), it is clear that the majority of lakes on the ice surface at Paakitsoq that are under 1300m elevation drain by the middle of August and any surface meltwater produced after this time drains straight into the en- and subglacial hydrological system (Thomsen et. al., 1988).

### 4.1.4. Implications of inland ice supraglacial hydrology on ice sheet dynamics

Surface lakes have the potential to drain large quantities of meltwater into the en- and subglacial hydrological system at vary timescales. The present study identified that in 2008, there were a number of lakes that were of substantial dimensions, that could have contributed enough water to the ice sheets hydrological system to potentially effect local and regional changes on ice sheet topography and flow dynamics (as described by Das et. al., 2008). It is not known, however, whether any of the drainage events that drained the large lakes identified in the present study did, in fact, cause such effects as described by Das and others (2008) as the absence of relevant, current literature suggests the Paakitsoq region was not the subject of glaciological research into the effects of surface lake drainage on ice sheet dynamics at this time.

## 4.2. Modeling supraglacial lake evolution at Paakitsoq

### 4.2.1. Initial test model run

The initial model run conducted for a 50 day period at the end of the melt season in 2007 for a pour point at 930m elevation gave results that indicated two forcing regimes that determined the production and supply of meltwater to a surface pour point on the DEM. The shorter fluctuation in modelled discharge, causing a saw-toothed pattern in the output graph (figure 15), is linked to diurnal variations in incoming solar radiation – greater insolation receipts during the day increases ice surface temperature and in turn causes more surface melting than during night time. This is accounted for in the model outputs as peaks in discharge (daytime discharge) and troughs in discharge (during the night). The longer fluctuations (shown as four distinct periods of discharge in figure 15) likely result from waves of meltwater produced as the ice sheet surface is melted in layers. Superimposed ice – layers of ice that have once had water percolating through them that has refrozen (Hooke, 2005, p.20) – forms layers and lenses of the ice sheet surface that require a certain amount of incoming shortwave radiation to melt them. When one of these ice lenses melts, a large volume of meltwater is produced, which is routed to the nearest moulin, and exposes a fresh ice lens that requires further insolation receipts to melt, thus limiting the production of meltwater for a period until the next ice lens is thawed and the same

process starts again. The model suggests that between large-scale oscillations the discharge into the pour point decreases to zero. This unlikely to be the case (Zwally et. al., 2007) unless on certain days the surface temperature of the ice is so low that no meltwater can be created – by investigating the MET data, this is unlikely to have occurred for the whole period that the model predicts zero meltwater discharge into the moulin as surface air temperatures are high enough to initiate melting (Colbeck, 1972).

The initial test run suggested that the surface energy balance submodel produced meltwater that was not routed to the pour point, and this suggests that the model may be capable of responding to external forcing mechanisms affecting the production of meltwater well, but that the surface routing submodel may be incapable of routing this meltwater efficiently to the desired moulin. The intensity of the peaks of modelled discharge are related to short periods of warming in the MET dataset and so the model does appear to respond to temperature fluctuations by increasing or decreasing the production of surface meltwater - with a coarse 500m x 500m DEM being used in the model runs, it is very likely that this is the reason for the model not producing more ‘accurate’ or ‘expected’ results, rather than the model not responding to meteorological forcing. This is discussed below in further sections of the present study.

The larger scale fluctuations in meltwater delivery to the pour point seen in figure 15 are thus related to the insolation dynamics affecting surface melt of the ice sheet. However, the model also accounts for delays in routing the surface meltwater to the pour point. In the case of the initial model run, this delay did not involve routing the meltwater through a snow pack (due to the lateness of the melt season, a snow pack was not provided as a model input as it likely would have been melted at this elevation, exposing superimposed ice layers that act as a pure ice surface – Hooke, 2005, p.21), although meltwater routing across a bare ice surface is also subject to delay based on the distance of meltwater production compared to the pour point. The long period oscillations in discharge are therefore also influenced by the length of time the produced surface meltwater takes to reach the pour point from all the cells in the watershed supplying the pour point with melt. The first, highest peak in the four oscillations is aided by the melting of the ice sheet close to the moulin, with the peak discharge being reached quickly because of melt waters close proximity to the moulin. The second rising limb, occurring shortly after the first is caused by

meltwater produced further from the moulin being delivered to the pour point. The extended falling limb of discharge is caused by the delivery of melt furthest from the pour point being received in lower and lower quantities.

### 4.2.2. Modelling lake *H*

Discharge into lake *H* occurred in two distinct periods separated by extended periods of no discharge. Although the periods of discharge exhibited limited diurnal fluctuation, and were not of a high value (the River Thames has a discharge of 65.4 cumecs, for example, while the modelled filling of lake *H* peaked at a discharge of 0.2 cumecs), they corresponded well with periods of higher temperatures in the MET data. Manipulated to develop a graph of lake volume evolution, the model outputs suggest that after an initial period of gradual filling, the filing rate of the lake increases greatly, due to the removal of the snowpack. This increased rate of filling occurs for around 30 days, and matches the rate of filling of the observed lake growth, but offset by a month and a factor of 10. The filling rate then decreases again as the ablation season begins to wane and temperatures begin to drop, preventing high surface melting rates like those observed in the MET data previously in the season.

Lake *H* has a medium sized watershed (of 16.4km$^2$) with 65.5 DEM cells creating meltwater that should flow to the pour point and produce extended hydrographs that provide discharge over a longer timescale than modelled (as the meltwater produced at the limits of the catchment is delayed in reaching the moulin instantaneously on being produced). However, model outputs suggest that over 10x10$^7$ m$^3$ of water produced over the model run was lost (did not enter the lake basin), and thus caused the model outputs to fall much below the volumes observed in, and estimated from the LandSat imagery on June 24$^{th}$ 2008. This excess modelled melt is likely to have run-off the ice sheet surface into another watershed (such as the watershed of lake *W* to the south) and thus contributed to another pour points modelled discharge – this possibility is discussed further below. However, this vast quantity of meltwater produced by the model exceeds observed meltwater production at the time of maximum lake volume shown in the June LandSat image, although after this date, melt rates may increase on the surface of the ice sheet (due to the warming of the climate with the onset of summer) and the volume of water draining into the

open moulin may begin to match the modelled results. As no data is known for the volumes of melt produced on the ice surface once lakes drain, it is difficult to say whether modelled rates of meltwater production exceed actual rates of meltwater production. Thus all that may be said is that modelled lake volume is much less than observed volume, but when the extra meltwater produced by the model is taken into account, the volume of lake *H* in June when the LandSat image was collected would far exceed the observed volume (by a factor of 10). The model therefore accounts for more water than is actually produced and routed to the observed lake, but fails to route this water as effectively as the actual supraglacial hydrological system present at Paakitsoq, resulting in model outputs that are far less than observed estimated volumes.

The model outputs suggest that more meltwater is produced on the surface of Paakitsoq than is observed to be routed into supraglacial lake *H*, and thus future research may be interested in measuring the ablation rate of the ice sheet surface in the lake catchment as identified during the watershed analysis, and using dye-tracing to investigate the total discharge into the lake, to see whether all the meltwater produced does indeed get routed to the lake. The present model suggests that this excess meltwater flows out of the watershed, and a number of supraglacial channels linking lakes on the ice surface are identifiable which may account for the loss of this excess meltwater elsewhere on the ice surface, if the model correctly predicts a higher melt rate than the volume observed lakes account for.

### 4.2.3. Modelling lake *J*

The hydrograph returned for lake J shows less diurnal fluctuation than the discharges modelled for lake H. This may be because the lake elevation is lower, and thus meteorological forcing is less varied (with generally higher temperatures throughout a daily cycle), allowing a more continuous process of surface ice melting throughout the peak in the hydrograph. The first peak in the hydrograph is the most pronounced and accounts for the greatest volume of water entering the lake. This peak is likely caused by the removal of the winter snowpack, but this would be unlikely to cause the greatest influx of water into an observed surface lake as bare ice melts at a greater rate than snow (due to the lower albedo of ice over snow), and so the first peak

is, in theory, anomalous. However, the watershed area that feeds the lake is very small (at just 19 DEM cells, or 4.8km$^2$) and thus the delay between meltwater production and routing to the lake is minimal. Any surface meltwater produced is likely to be swiftly routed to the pour point, and the melting of the winter snowpack, with a high snow water equivalent compared to the melting of layers of ice lenses (Colbeck, 1972; Hooke, 2005, p.20-22) is thus capable of producing a greater peak in discharge into the lake over a smaller area catchment than in a large-scale catchment area.

The second peak in the hydrograph is then likely caused by the melting of ice lenses across the catchment (as total insolation rates exceed the threshold needed to melt a particular layer of ice), with the short routing delay causing the meltwater to enter the lake basin rapidly and cause a 'flashy' hydrograph with a steep rising and falling limb. The third peak is composed of a short period of much lower discharges into the pour point, and is later in the melt season, suggesting that the melt season may be beginning to wane at this elevation and that the insolation receipts struggle to cause full ice lens melting as they did earlier in the melt season.

However, the model produced a vast quantity of meltwater that was not routed to the pour point (exceeding 30x10$^7$ m$^3$), and this meltwater discharge was prolonged across the ablation season. This excess meltwater, had it been routed adequately to the pour point would have caused the volumetric evolution of the lake to exceed the observed estimated volume at it's maximum dimensions, and thus again, the model suggests a melt rate of the ice surface that is far greater than observed from the LandSat imagery collected in 2008. Further investigation and field study on the ice surface at Paakitsoq would aid the present study by calculating the actual melt rate on the ice sheet in the region and then comparing this volume of water produced with the volume modelled – presently, comparing modelled volumes with estimated observed volumes pre-lake drainage mean adequate conclusions about the accuracy of the model used in the present study can be suggested, but hard to define.

### 4.2.4. Modelling lake *W*

Lake *W* exhibited the most realistic modelled volumetric evolution compared to the estimated observed lake evolution, and the modelled hydrograph reflects this. Diurnal fluctuations in meltwater discharge into the pour point were closely related to

the MET data and showed the numerical model could accurately predict the forcing of the regional climate on melt rates at Paakitsoq. The two peaks of meltwater discharge into the pour point represent the initial melting of the snowpack (the first, lower peak in discharge), and then the melting of the bare ice surface (the second, greater peak in discharge) as would be expected (as suggested by Hooke, 2001, p.20; McMillan et. al., 2007; Long, MPhil dissertation) at this elevation at the respective times in the ablation season. The receding limb of each peak is longer than the other modelled lake input discharges and is caused by lake *W*s large catchment area (of 141.9 DEM cells, or 35.5km$^2$) ensuring a delay between the initial meltwater close to the moulin being routed to the pour point, and the meltwater created furthest from the moulin being routed to the pour point. Further, as the catchment for lake *W* was identified by the static DEM analysis as being linked to the catchment for lake *H* (see figure 1C in Appendix A), it is likely that some excess water from the linked catchment was fed into the lake *W* catchment, and an even greater delay between meltwater production and routing to the pour point is experienced (thus prolonging the period of lake filling at low discharges).

Although the model deals with greater filing rates as the ablation season progresses (reflected in the increase in estimated filling rates of the observed lake), it does not suggest the correct increase in filing rate that the observed lake suggests. This is likely due to the loss of meltwater form the modelled catchment that is produced in the model, but not routed to the pour point. As with lake *H* and *J*, lake *W*s catchment was modelled to produce some 28x10$^7$ m$^3$ of meltwater which was not routed to the pour point. Had this been routed to the lake, the model overestimated melt rates in the catchment by a huge amount, and would have led to the modelled lake reaching its maximum observed volume far earlier than it did in reality (within 5 days of the model being run, compared to around 80 days after the beginning of the model run as observed on the ice sheet surface).

### 4.2.5. Lake drainage

Lake drainage is observed throughout the melt season on the ice surface as identified in the satellite images. However, the numerical model employed in the present study does not account for an ice dammed lake that fills and subsequently

drains, rather it accounts for the discharge into an open moulin. This is not problematic for model results, as data manipulation enables theoretical lake volumes to be calculated, however lake drainage is a problem in the observed LandSat images, as once a lake drains, it is impossible to measure how much actual meltwater is then being routed to the open moulin. This is a limitation of the present study and future study is likely to require fieldwork on the ice surface to determine actual melt rates in lake catchments post lake drainage.

### 4.2.6. Implications of model results on ice sheet dynamics

Model results suggest that not enough meltwater is routed to the identified moulins to produce any substantial effects on ice sheet flow regimes or local dynamics. If lakes *H*, *J* and *W* filled with modelled discharge to the corresponding date of observed maximum volume (although this may not represent the real maximum volume due to the LandSat image being temporally constrained), upon lake drainage, a much smaller quantity of meltwater than observed would be inputted into the en- and subglacial hydrological system, and it is doubtful if such low volumes of water would be able to hydraulically pressurize the subglacial system and cause flow anomalies and local topographic uplift as described by Das and others (2008) in the vicinity of the surface lake location. However, if all the modelled discharge is taken into account, it is likely that the lakes produced by the model would cause large scale flow variation and local topographic uplift, as the volumes concerned far exceed observed volumes from the satellite imagery collected in 2008. Further, it is likely that the volumes of water suggested by the present model could impact upon the inland ice subglacial drainage system as proposed by Long (MPhil dissertation), and potentially cause a channelized subglacial hydrological morphology (after Fountain and Walder, 1998) under the inland ice due to the constant high flux of water draining from the ice surface throughout the melt season, compared to the distributed system currently proposed. This implication is unlikely to manifest itself under the inland ice of great ice sheets (such as the Greenland Ice Sheet) as, in reality, the flux of water is too little to keep a channelized system functioning through the whole of the ablation season, as the system must adapt from being almost dormant during the accumulation season (and taking the form of a distributed subglacial morphology – Fountian and

Walder, 1998). Thus as yet, the model results do not prove or disprove previous suggested subglacial morphological theories under the inland ice at Paakitsoq, and further model testing is suggested to constrain model outputs to be more representative of observed meltwater patterns before conclusions be drawn as to the implications of model outputs on Greenland Ice Sheet dynamics.

### 4.3. Implications for the accuracy of the present model

The model used in the present study is most likely to be unrealistic where modelled hydrographs do not correlate well with observed data from previous studies on the Paakitsoq region, or with data collected for the present study in 2008. When the modelled melt routed to the pour point is calculated, model outputs are much less than the observed meltwater volumes on the inland ice surface, while the modelled meltwater volume that is generated in each lake catchment that is not routed to the pour point far exceeds the observed volume. This is likely a reflection of the limitation of the DEM to produce an accurate representation of the ice surface at Paakitsoq (as is discussed further below), but as this DEM is currently the only available elevation model of the region, it is still possible for future studies to develop the surface energy balance model to try and generate more accurate supraglacial melt rates than currently modelled.

#### 4.3.1. Implications of the surface energy balance model: limited modelled melt at the pour point

Even if the DEM is responsible for not routing enough of the modelled melt to the pour point, more melt might be produced by the energy balance model subroutine, by the provision of more representative MET data. Sensitivity tests suggest that the model responds greatly to increases in air temperature values, and that a potential increase of around 2°C could provide more representative modelled rates of meltwater discharge at the pour point (although this also increases the melt rate over the lake catchment area and thus the amount of extraneous melt that is lost from the DEM surface). However, for the first 50 days of the model run, the model fails to produce as much melt as the observations from LandSat imagery suggest occurs on the ice

surface and subsequently plays ‘catch-up’ (such as observed in the model run for lake *W*) and seemingly over-predicts the melt rate of the ice surface towards the end of the ice surface. This implies that the model is dampened excessively by snow-cover and then increases the melt rate of bare ice to a much greater degree. The model therefore may benefit from increased knowledge about the type of snow that falls over Paakitsoq (and the density of it by the end of the melt season) and the albedo of both the snow and the ice in region. These input data then exert a control on the cloudiness algorithm that relates to the incoming shortwave radiation receipts the force the surface melting routine, and if the snow density and albedo values were more representative of the ice surface values at Paakitsoq, rather than generic values, the melt rates produced by the model may be more representative of actual melt rates.

The author suggests, however, that improving the accuracy of the modelled meltwater discharges at the pour point is not as important as improving the quality of the DEM surface and enabling all the modelled meltwater to be routed to the pour point. In reality, the numerical model *does* over-predict the melt rate for the ice surface at Paakitsoq and thus the model may need to be dampened to meteorological forcing to prevent these excessive melt rates in future model runs.

### 4.3.2. Implications of the surface energy balance model: excessive modelled melting

The surface energy balance model creates too little melt when the surface routing model is employed to route the meltwater to the pour point. This limited melt can still be explained in terms of the model being forced by meteorological factors, and responding to diurnal fluctuations in air temperature, the melting of the snowpack, and the routing of the meltwater across the surface of the ice (and subsequent delay in discharge events), but, when the whole meltwater volume produced by the model is taken into account, lake volumes would far exceed the observed volumes, and the lack of correlation between observed and modelled meltwater production suggests that the model over-predicts the amount of meltwater is in fact produced on the ice surface at Paakitsoq in the melt season of 2008.

The present study could be aided by fieldwork on the surface of the inland ice at Paakitsoq to determine actual ablation rates during the melt season, and then to

improve the numerical model energy balance subroutine to model more accurately the amount of meltwater is produced at the surface and match modelled with observed results. It is impossible to estimate from the satellite imagery how much meltwater is produced in lake catchments when the lakes start to drain (as it is impossible to know how fast the lakes are draining, and how fast they are still being fed by meltwater) and thus the model may accurately deal with such meltwater production, but it is likely that the model *does* over-predict meltwater volumes throughout the melt season.

Initial sensitivity tests suggested that for lower elevations (between 900-950m), melt was produced from the very beginning of 2008 (January 1st), when the ice sheet is, in reality, snow covered and too cold to experience surface melting. With the response of the model to observed meteorological forcing, especially temperature, it is suggested that the model could be altered to dampen the effect of temperature on model outputs, by introducing a better relationship for albedo between snow and ice than is currently employed (after Arnold et. al., 1998), by including a cloudiness algorithm (derived from fieldwork studies) that is spatially constrained to Greenland and by investigating the influence of differing snow depths across the model area as opposed to conducting model runs assuming continuous start of season snow depth across the whole region, regardless of any actual variation observed from field studies or through theory of how snow cover varies spatially and temporally with elevation and location on the Paakitsoq inland ice. The model is thus often limited by its input data and this is discussed further below.

### 4.3.3. Implications of the DEM: excessive modelled melting yet ineffective model routing

As discussed above, the numerical model produces lake input hydrographs that cause lake volume evolution to fall much below that observed in the LandSat images. However, the model produces a large amount of meltwater that is lost over the DEM surface and not routed to the pour point identified in the model inputs. This is most probably due to the DEM surface being interpolated from LiDAR data at a coarse resolution of 500m x 500m (Toby Benham, personal communication, 4th June 2009).

LiDAR survey modules, although commonly used in DEM construction are still undergoing technological development (Flood, 2001) and data often return

breaklines and uniform elevation surfaces between a series of data points (Liu, 2008) that are then transferred in the interpolation process to the DEM surface, even when a high resolution DEM is being created. On creation of low-resolution DEMs, such as that used in the present study, these interpolation errors can manifest themselves as smoothed surfaces, ridged surfaces or surfaces that do not properly reflect topographic slope direction changes (Lohr, 1998). In the DEM surface used in the present study, the static surface hydrological analysis suggested that the DEM surface did not present any of these inherited errors from interpolation process, and that even the coarse resolution of the DEM could resolve some supraglacial channels that correlated well with observed surface channels that feed supraglacial lakes, albeit at a larger scale than the observed surface channels. However, small channels and topographic minima identified in some of the 2008 LandSat images and in previous studies (such as those by Thomsen et. al., 1988 and Long, MPhil dissertation) are unable to be resolved by the DEM, and thus rather than routing the modelled meltwater into supraglacial lakes, the model allows meltwater to simply run off the DEM surface and become lost to the inputted lake catchment.

It is suggested that a higher resolution DEM will be able to capture more of the modelled water and route it successfully to the pour point identified as an actual moulin. The model was written to utilise a DEM with 20m x 20m resolution (Arnold et. al., 1998), and thus if a higher resolution DEM were available for the ice sheet at Paakitsoq, future tests could be conducted to investigate the implications of the DEM resolution on model outputs.

A DEM with resolution of 100m x 100m is likely to have a great impact on modelled results as such a DEM would be able to resolve many more supraglacial hydrological features identified on LandSat images (such as smaller lakes, large crevasses and a variety of surface stream structures) and thus be more representative of the actual ice surface. Further, a particular aspect of the supraglacial hydrological system that is hard to model accurately is the location of sinks in the static hydrological analysis. This has implications for the ability to model both small and large lakes that appear on the surface of the ice sheet each year – currently the DEM fails to resolve identified moulins towards the ice marginal areas, and also at higher elevations where larger lakes form (filling through the June 2008 satellite image to great extents in the July 2008 image). As the DEM fails to resolve moulins in this region, an accurate comparison is currently impossible between meltwater production and routing to large

lakes around 1000m elevation that drain after the June image and those lakes that are located at above 1200m elevation and keep filling after the June image, only draining by the August image. A higher resolution DEM would be able to resolve topographic minima to a greater extent and thus improve the ability of the model to differentiate between marginal surface hydrological systems and inland ice supraglacial hydrology as identified from the 2008 satellite images. Similarly, it would be able to increase the number of sinks identified in the static surface hydrological analysis, which would increase the number of sinks inputted into the model and allow a greater range of lakes to be modelled through the ablation season. This increase in the number of results would allow trends to be identified that are more representative of the observed hydrological features (after Johannesson and Cressie, 2004). As has been shown in the present study, the ice surface at Paakitsoq, although dynamic, does not change much over decadal timescales as the individual hydrologic features often maintain a local position on the ice surface across a number of years, and thus an upgraded resolution DEM could be used for many years worth of future study before becoming obsolete.

### 4.4. Limitations of the present model

The present model takes into account a variety of factors that influence supraglacial lake inception and evolution on the Greenland Ice Sheet, such as the varying flow-delaying mechanisms associated with a snow pack, or bare ice surface, and the influence of a variety of meteorological factors on meltwater production. Certain elements of the supraglacial hydrological cycle, however, remain excluded. Other considerations would strengthen model outputs: the introduction of a sub-model that represents lake flow regimes would aid the ability of the model to more accurately represent the evolution of supraglacial water bodies as lake currents may influence melt rates at the lake margins and add to lake volume; the introduction of a more advanced surface routing component that allows the superposition of observed surface channels into the model (either in the static hydrological analysis, or in the numerical model itself) as this is likely to lead to more accurate melt water routing across the ice sheet surface than the standard D8 SFD component utilized in ArcView 3.3 and the model itself; the introduction of a sub-routine that deals with the ablation of the ice surface under filled lakes – Luthje and others (2006) identify that ablation is

enhanced by 110-170% under supraglacial lakes compared to bare ice, and this process increases with the depth of lake and decreases with elevation, and so is an important feedback mechanism that can increase lake volume but is rarely considered in current models of supraglacial lake evolution.

The present study does not allow lakes to over flow their basins (and potentially to provide melt water inputs into other lake basins upon lake 'overflow') as the hydrographs produced in the model represent water flux into an open moulin, rather than discharge inputted into a constrained basin (constrained by an ice dam and the limited volume of individual basins, as shown in figure 9 and discussed in the results section). Adaptations of the model could include the addition of numerical code that deals with individual ice-dammed lake basins, as defined by the static hydrological analysis on the DEM and the available LandSat imagery, and can therefore account for lakes that overspill when they reach their suggested maximum volumes (consequently releasing excess meltwater into other watersheds).

Precipitation data for Paakitsoq are not available, and precipitation data for Greenland as a whole are not widely available or easy to collect (Dethloff et. al., 2002). Limited data was collected by Omhura and Reeh (1991) to interpolate a precipitation and accumulation map of the whole of the Greenland Ice Sheet, but in the light of climate warming, this dataset is limited in its application to current investigation of the ice sheet. In the summer melt season when surface lake inception and evolution takes place, the Paakitsoq region does not normally experience large precipitation inputs due to it's location on Greenland and due to the fact that in this region, Icelandic cyclones are prevalent and are not favourable for precipitation (Chen et. al., 1997). Therefore the present study having been conducted without precipitation inputs into numerical model runs is unlikely to have unduly affected modelled hydrographs of surface meltwater production and routing to surface sinks on the ice sheet. However, occasionally, lee cyclogenesis over the southern extent of the Greenland Ice Sheet as described by Chen and others (1997) causes cyclones to travel up the western coastline towards the Paakitsoq region, and provide precipitation over short timescales to the west coastal margins of the ice sheet. A regional climate model, such as the HIRHAM4 model discussed by Dethloff and others (2002; also Dethloff et. al., 1996), could be coupled to the present numerical model to provide precipitation inputs at high spatial and temporal resolution, and could also deal with

air temperatures, wind speed and direction, and snowpack evolution. Such a model could potentially replace the energy balance sub-model.

Although the addition of these sub-components would be desirable for future investigation into supraglacial lake evolution on the Greenland Ice Sheet surface around Paakitsoq, the main limitation of the model identified by the author is still the DEM. With a higher resolution DEM, the model results may be different, and likely more reflective of the melting and filling regimes of the suite of hydrological features identified yearly on the ice surface at Paakitsoq.

## 5. Conclusions

The surface energy balance model used in the present study is the most complex model to have been applied to the surface of the Greenland Ice Sheet at Paakitsoq (after Knight, 2004, p.36) and combined with a meltwater routing submodel has provided the study with a series of data from which conclusions can be drawn. The surface energy balance model has developed diverse results, suggesting that at higher elevations, the modelled rates of filling of supraglacial lakes, although much lower in volume to observed lake filling, can match the apparent inter-seasonal patterns of observed lake evolution, whereas at lower elevations, these patterns are less easy to model. Further, the impact of lake basin elevation, meteorological forcing, and the delay in meltwater routing provided by the melt routing submodel can all be applied successfully to the production and routing of meltwater on ice sheet surface and provide results that show a correlation with observed patterns as identified in the LandSat imagery collected for the study period.

However, the model is limited in the input data that are available to run it, and this affects the model results as identified through initial test runs, sensitivity tests, static hydrological analysis and observed lake evolution on the ice sheet surface as seen in the LandSat imagery. Large quantities of meltwater are generated by the model, but fail to be routed to the pour point – this limits the models ability to produce the observed lake volumes and thus limits the number of conclusions that are able to be drawn regarding the investigation into the evolution of surface lakes by a numerical model.

Lake evolution in 2008 can be investigated, however, by an examination of the LandSat imagery collected in 2008. There is a notable difference between ice marginal and inland ice hydrological systems, and the results show that the supraglacial hydrological system migrates inland as the melt season progresses, with larger lakes forming throughout the melt season at higher elevations. These lakes form in similar locations every year, and show a high correlation between their locations in 2008 and with data available from 2001 and 1988. Combined with model outputs, and observed lake evolution regimes derived from the satellite imagery, filling regimes for surface lakes can be estimated, and the potential effects of these lakes draining on ice sheet dynamics can be proposed.

The numerical model used in the present study would undoubtedly benefit from further use and refining. As supraglacial lakes play an important part in the hydrological cycle of ice sheets and can cause flow regime alterations that influence ice flux dynamics at the ice sheet margins, in a warming world, their influence is ever increasing. As global climate warms, the region that these lakes occupy will increase as snow lines retreat inland and the surface slopes at higher elevations decrease allowing larger and larger lakes to form (Luthje et. al., 2006). Numerical modelling of the lake volumes involved would be invaluable in determining meltwater inputs into the en- and subglacial hydrological system, and understanding better how this meltwater can influence ice sheet flow dynamics. The present study has begun this investigation and suggests there is a long way to go before supraglacial lake evolution can be modelled accurately at Paakitsoq, mainly because the inputs into the current model are not based on accurate measurements taken in the field at this location. Field measurements are difficult and expensive (Painter et. al., 2007), but in order to more accurately model the effects of climate warming on an ice mass that has the capacity to raise global sea levels by over 6.5m, the author believes the time, effort and expense is worth it to provide invaluable model inputs that will aid future investigation into supraglacial lake evolution on the surface of the Greenland Ice Sheet.

# References


Ahlstrøm, A.P. 2007. Previous glaciological activities related to hydropower at Paakitsoq, Ilulissat, West Greenland. *Danmarks og Grønlands Geologiske Undersøgelse Rapport 2007/25*.

Arnold, N., Willis, I.C., Sharp, M.J., Richards, K.S., Lawson, W.J., 1996. A distributed surface energy balance model for a small valley glacier. I. Development and testing for Haut Glacier d'Arolla, Valais, Switzerland. *Journal of Glaciology*, **42**, 77-89.

Arnold, N., Richrads, K., Willis, I., Sharp, M., 1998. Initial results from a distributed, physically based model of glacier hydrology. *Hydrological Processes*, **12**, 191-219.

Bamber, J.L., Alley, R.B., Joughin, I., 2007. Rapid response of modern day ice sheets to external forcing. *Earth and Planetary Science Letters*, **257**, 1-13.

Boon, S. and Sharp, M., 2003. The role of hydrologically-driven ice fracture in drainage system evolution on an Arctic glacier. *Geophysical Research Letters, **30** (18), 16-19.*

Chen, J.L., Wilson, C.R., Tapley, B.D., 2006. Satellite Gravity Measurements Confirm Accelerated Greenland Ice Sheet. *Science*, **313**, 1958-1960.

Chen Q.S., Bromwich, D.H., Bai, L., 1997. Precipitation over Greenland retrieved by a dynamic method and its relation to cyclonic activity. *Journal of Climate*, **10**, 839–870.

Chikita, K., Jha, J., Yamada, T., 1999. Hydrodynamics of a Supraglacial Lake and Its Effect on the Basin Expansion: Tsho Rolpa, Rolwaling Valley, Nepal Himalaya. *Arctic, Antarctic, and Alpine Research*, **31** (1), 58-70.

Colbeck, S.C., 1972. A theory of water percolation in snow. *Journal of Glaciology*, **11**, 369-385.

Colbeck, S.C., 1978. The physical aspects of water flow through snow. In: V. T. Chow (ed.), 1978, *Advances in Hydroscience, Volume 11*, Academic Press, New York, N.Y., 165-206.

Das, S.B., Joughin, I., Behn, M.D., Howat, I.M., King, M.A., Lizarralde, D., Bhatia, M.P., 2008. Fracture propagation to the base of the Greenland Ice Sheet during supraglacial lake drainage. *Science,* **320**, 778-781.

Dethloff K., Rinke, A., Lehmann, R., Christensen, J.H., Botzet, M., Machenhauer, B., 1996. Regional climate model of the Arctic atmosphere. *Journal of Geophysical Research*, **101**, 23401–23422.

Dethloff, K., Schwager, M., Christensen, J.H., Kiilsholm, S., Rinke, A., Dorn, W., Jung-Rothenhäusler, F., Fischer, H., Kipfstuhl, S., Miller, H., 2002. Recent Greenland accumulation estimated from regional climate model simulations and ice core analysis. *Journal of Climate*, **15** (19), 2821-2832.

Echelmeyer, K., Clarke, T.S., Harrison, W.D., 1991. Surficial glaciology of Jakobshavns Isbrae, West Greenland. *Journal of Glaciology*, **37**, 368–382.

Flood, M., 2001. Laser altimetry - from science to commercial lidar mapping. *Photogrammetric Engineering and Remote Sensing*, **67** (11), 1209-1211, 1213-1217.

Fountain, A.G., Walder, J.S., 1998. Water flow through temperate glaciers. *Reviews of Geophysics*, **36** (3), 299-328.

GEUS Ilulissat Icefjord article: http://www.geus.dk/viden_om/voii/ilulissat-uk/voii06-uk.html. Last accessed - 29th April 2009

Gregory, J.M., Huybrechts, P., Raper S.C.B. 2004. Climatology: Threatened loss of the Greenland ice-sheet. Brief Communications, *Nature*, **428**, 616.

Gulley, J., Benn D.I., 2007. Structural control of englacial drainage systems in Himalayan debris-covered. *Journal of Glaciology*, **53** (182), 399-412

Holmlund, P., 1988. Internal geometry and evolution of moulins, Storglaciären, Sweden. *Journal of Glaciology*, **112**, 242-248.

Hooke, R.LeB., 2005. *Principles of Glacier Mechanics* (2nd Edition: illustrated and revised). Cambridge University Press, England, 429p.

Howat, I.M., Joughin, I., Scambos, T.A., 2007. Rapid Changes in Ice Discharge from Greenland Outlet Glaciers. *Science*, **315** (5818), 1559-1561.

Jansson, P., Hock, R., Schneider, T., 2003. The concept of glacier storage: a review. *Journal of Hydrology*, **282,** 116-129.

Jezek, K.C., Drinkwater, M.R., Crawford, J.P., Bindschadler, R., Kwok, R., 1993. Analysis of synthetic aperture radar data collected over the southwestern Greenland ice sheet. *Journal of Glaciology*, **39** (131), 119-132.

Johannesson, G., Cressie, N., 2004. Finding large-scale spatial trends in massive, global, environmental datasets. *EnvironMetrics*, **15** (1), 1-44.

Kenny, F., Matthews, B., 2005. A methodology for aligning raster flow direction data with photogrammetrically mapped hydrology. *Computers and Geosciences*, **31** (6), 768-779.

Knight, P.G, 1999. *Glaciers*. Routledge, Chichester (London), 271 pages.

Knighton, A.D., 1972. Meandering habit of supraglacial streams. *Geological Society of America Bulletin*, **83**, 201-204.

Kosiba, A., Loewe, F., 1964. Meteorolgical observations in the Tasersiaq Area, Southwest Greenland, during summer, 1963. *Institute of Polar Studies*, Report Number 11 (rf 1701).

Kostrzewski A., Zwoliñski Z.B., 1995. Hydraulic geometry of a supraglacial stream. *Quaestiones Geographicae*, Special Issue **4**, Adam Mickiewicz University Press, Poznañ, 165-176 (also accessible at: http://www.staff.amu.edu.pl/~zbzw/gh/gh9.htm - last accessed 4th April 2009, 6.36pm BST).

Krabill, W., Hanna, E., Huybrechts, P., Abdalati, W., Cappelen, J., Csatho, B., Frederick, E., Manizade, S., Martin, C., Sonntag, J., Swift, R., Thomas, R., Yungel, J., 2004. Greenland Ice Sheet: Increased coastal thinning. *Geophysical Research Letters*, **31**.
Boon, S. and Sharp, M. 2003. The role of hydrologically-driven ice fracture in drainage system evolution on an Arctic glacier. *Geophysical Research Letters*, **30** (18), 1916.

Liu, X., 2008. Airborne LiDAR for DEM generation: some critical issues. *Progress in Physical Geography*, **32** (1), 31-49.

Lohr, U., 1998. Digital elevation models by laser scanning. *Photogrammetric Record*, **16**, 105-109.

Long, S., 2008. Subglacial meltwater drainage at Paakitsoq, West Greenland: insights from a distributed physically based numerical model. *MPhil dissertation*, University of Cambridge, 88pp.

Luthje, M., Pedersen, L.T., Reeh, N., Greuell, W., 2006. Modelling the evolution of supraglacial lakes on the West Greenland ice-sheet margin. *Journal of Glaciology*, **52** (179), 508-518.

Marston, R.A., 1983. Supraglacial stream dynamics on the Juneau Icefield. *Annals of the Association of American Geographers*, **73**, 597-608.

Maurer, J., 2006. Local-scale snow accumulation variability on the Greenland Ice Sheet from ground penetrating radar. *Masters Thesis*, University of Colorado at Boulder.

Meier, M.F., Dyurgerov, M.B., Ursula, R.K., O'Neel, W.S., Pfeffer, T.,
Anderson, R.S., Anderson, S.P., Glazovsky, A.F., 2007. Glaciers Dominate Eustatic Sea-Level Rise in the 21st Century. *Science*, **317**, 1064-1067.

McMillan, M., Nienow, P., Shepherd, A., Benham, T., Sole, A. 2007. Seasonal evolution of supra-glacial lakes on the Greenland Ice Sheet. *Earth and Planetary Science Letters*, **262**, 484-492.

Mernild, S.H., 2006. The internal drainage system of the lower Mittivakkat Glacier, Ammassalik Island, SE Greenland. *Geografisk Tidsskrift (Danish Journal of Geography)*, **106** (1), 13-24.

Oerlemans, J., 1992. Climate sensitivity of glaciers in Southern Norway: application of an energy balance model to Nigardsbreen,Hellstugbreen and Alfotbreen. *Journal of Glaciology*, **38**, 223-232.

Oerlemans, J., 1993. A model for the surface balance of ice masses: part 1. Alpine glaciers. *Zeitschrift für GletscherKunde und Glazialgeologie*, **27/28**, 63-83.

Oerlemans, J., Bassford, R.P., Chapman, W., Dowdeswell, J.A., Glazovsky, A.F., Hagen, J.-0., Melvold, K., De Ruyter De Wildt, M., van de Wal, R.S.W., 2005. Estimating the contribution of Arctic glaciers to sea-level change in the next 100 years. *Annals of Glaciology*, **42**, 230-236.

Oerlemans, J., Dyurgerov, M., van de Wal, R.S.W., 2007. Reconstructing the glacier contribution to sea-level rise back to 1850. *The Cryosphere*, **1**, 59-65.
Ohmura A., Reeh, N., 1991. New precipitation and accumulation maps for Greenland. *Journal of Glaciology*, **37**, 140–148.

Painter, T.H., Molotoch, N.P., Cassidy, M., Planner, M., Steffen, K., 2007. Contact spectroscopy for determination of stratigraphy of snow optical grain size. *Journal of Glaciology*: Instruments and Methods, **53** (180), 121-127.

Rignot, E., Kanagaratnam, P., 2006. Changes in the Velocity Structure of the Greenland Ice Sheet. *Science*, **311**, 986-990.

Sneed, W.A., Hamilton, G.S., 2007. Evolution of melt pond volume on the surface of the Greenland Ice Sheet. *Geophysical Research Letters*, **34**, 1-4.

Shepherd, A., Wingham, D., 2007. Recent Sea-Level Contributions of the Antarctic and Greenland Ice Sheets. *Science*, **315**, 1529-1532.

Sneed,W.A., Hamilton, G.S., 2007. Evolution of melt pond volume on the surface of the Greenland Ice Sheet. *Geophysical Research Letters*, **34**, L03501

Steffen, K., Box, J.E., Abdalati, W., 1996. Greenland Climate Network: GC-Net. *US Army Cold Regions Reattach and Engineering (CRREL), CRREL monograph*, trib. to M. Meier.

Steffen, K. and Box, J. 2001. Surface climatology of the Greenland ice sheet: Greenland climate network 1995-1999. *Journal of Geophysical Research – Atmospheres*, **106**,
33951-33964.

Stenborg, T., 1970. Delay of runoff from a glacier basin. *Geografiska Annaler*, **52A**, 1-30.

Stober, M., Hepperle, J., 2006. Changes in ice elevation and ice-flow velocity in the Swiss Camp area (West Greenland) between 1991 and 2006. *Polarforschung*, **76** (3), 109-118.

Thomsen, H.H. and Reeh, N. 1986. Glaciological investigations at the margin of the Inland Ice north-east of Jakobshavn, West Greenland. *Rapport Grønlands Geologiske Undersøgelse*, 130, 102-108.

Thomsen, H.H., Braithwaite, R.J. 1987. Use of remote-sensing data in modelling run-off from the Greenland Ice Sheet. *Annals of Glaciology*, **9**, 1-3.

Thomsen, H.H., Thorning, L., Braithwaite, R.J. 1988. Glacier-hydrological conditions on the Inland Ice north-east of Jakobshavn/Ilulissat, West Greenland. *Rapport Grønlands Geologiske Undersøgelse*, **138**, map with text.

Thomsen, H.H., Thorning, L., and Olesen, O.B. 1989b. Applied glacier research for planning hydro-electric power, Ilulissat/Jakobshavn, West Greenland. *Annals of Glaciology*, **13**, 257-261.

van de Wal, R.S.W., Boot, W., van den Broeke, M.R., Smeets, C.J.P.P., Reijmer, C.H., Donker, J.J.A., Oerlemans, J., 2008. Large and Rapid Melt-Induced Velocity Changes in the Ablation Zone of the Greenland Ice Sheet. *Science*, **321**, 111-113.

Watanabe, T., Kameyama, S., Sato, T., 1995. Imja Glacier dead-ice melt rates and changes in a Supra-Glacial Lake, 1989-1994, Khumbu Himal, Nepal: Danger of Lake Drainage. *Mountain Research and Development*, **15** (4), 293-300.

Wessels, R.L, Kargel, J.S., Kieffer, H.H., 2002. ASTER measurement of supraglacial lakes in the Mount Everest region of the Himalaya. *Annals of Glaciology*, **34**, 399-408.

Willis, I., Arnold, N., Brock, B., 2002. Effect of snowpack removal on energy balance, melt and runoff in a small supraglacial catchment. *Hydrological Processes*, **16**, 2721-2749.

Zwally, H.J., Abdalati, W., Herring, T., Larson, K., Saba, J., and Steffen, K. 2002. Surface melt-induced acceleration of Greenland ice-sheet flow. *Science*, **297**, 218-222.

# Appendix A: Supplementary methods

## Static drainage routing analysis

Supraglacial flow routes were analysed using the 500m pixel resolution surface DEM (figure 1B below) of the Paakitsoq region in ArcView 3.3 software. The Spatial Analyst extension was loaded and the toolbox employed, so other sub-functions could be utilised. The procedure used was as follows:

- Using the *flow direction* tool, flow direction was calculated for each cell. Flow from each cell is directed to a downstream cell determined by the surrounding cell with the lowest elevation (in one of eight possible directions following the D8 SFD method). The flow direction output for the Paakitsoq DEM is given below (figure 1A).

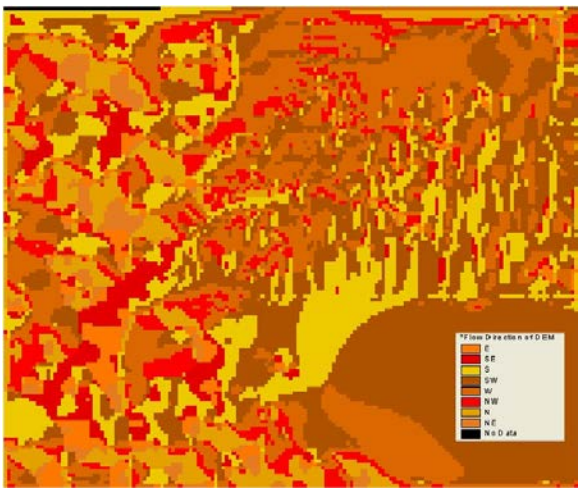


**Figure 1A: Flow direction output visualized in ArcView 3.3, showing the flow direction of theoretical water inputs across the surface of the Paakitsoq region DEM used in the present study. Interpolation errors when the DEM was being created cause areas of the elevation model to exhibit uniform flow direction. In reality local topographic deviation at the sub-DEM resolution scale will cause small scale supraglacial flow variations that cannot be resolved by the static drainage routing function on such a coarse DEM, and thus uniform flow direction prevails.**

- Using the *sink* tool, sinks in the surface DEM were identified for the flow direction input as produced above, with cells receiving flow from all surrounding cells.
- Using the *flow accumulation* tool, the number of upstream cells flowing to each cell could be calculated.
- Using the *watershed* tool, a map of the entire supraglacial catchment contributing to a specific sink was created (as shown in figure 1B below).

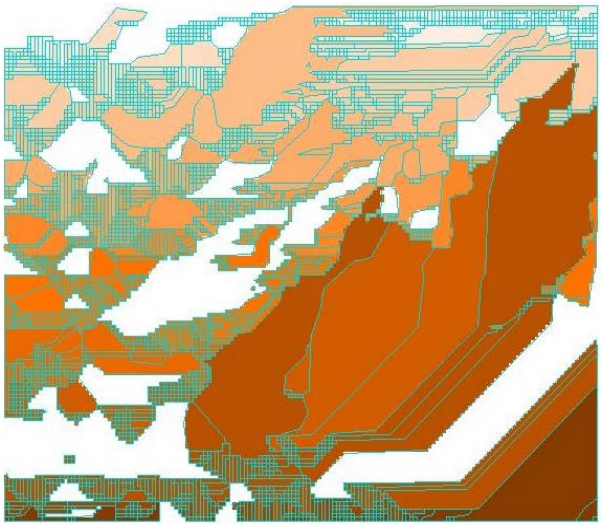

**Figure 1B: Supraglacial watersheds identified for the Paakitsoq region in ArcView 3.3. Areas corresponding to uniform flow direction exhibit large, anomalous watersheds due to the errors incurred in the DEM during the kriging and interpolation process (as discussed above). However, in these areas, only one sink was identified during ice surface static hydrological analysis.**

- Once the watersheds for the supraglacial study area were identified, the sinks were overlaid onto the watershed surface in ArcView 3.3 and the watersheds of sinks *H*, *J*, and *W* (and a further lake to the north east of these lakes) discussed in the present study were identified. These watersheds are shown in figure 1C, and their vital statistics were computed within ERDAS Imagine 9.0 software:

**Figure 1C: Watersheds identified for four lakes discussed above, as determined by the static supraglacial flow routing analysis. Surface areas were determined for each of the watersheds shown – lake H's watershed (pink) constituted 65.5 DEM cells, equating to 42.2km$^2$; lake J's watershed (blue) contained 19 DEM cells, with an area of 4.8km$^2$; lake W's watershed (green) is composed of 141.9 DEM cells, with an area of 35.5km$^2$.**

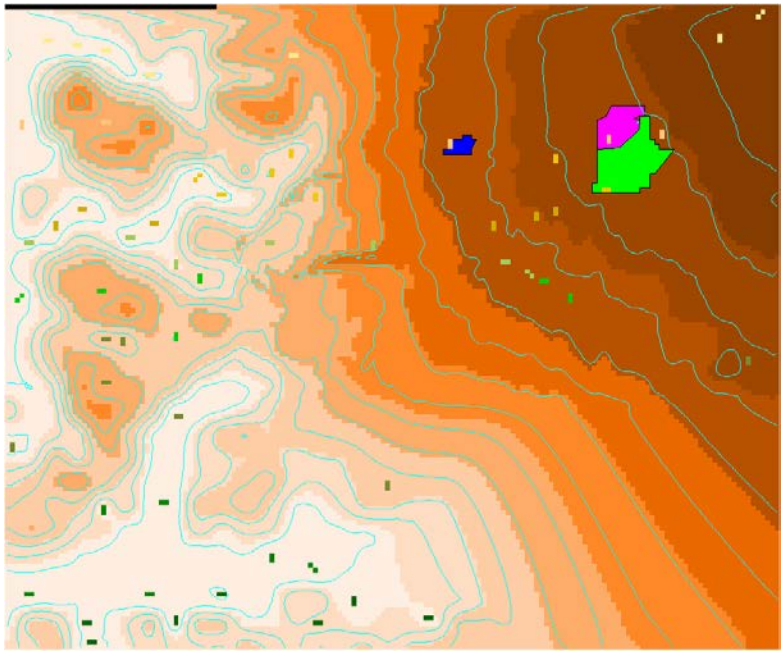

# Appendix B: Supplementary data

## DEM manipulation

The DEM used in the static drainage routing analysis described above, and in the initial numerical model runs is shown in figure 8, and measured 80.5km by 67km. This DEM extent was later modified to represent a rough 'cut' of the ice surface from the margin of the ice sheet to the inland ice extent covered by the initial DEM. This cut was performed by manipulating and visualizing the topographic dataset in Matlab R2006b statistical mathematics software package, and creating an ice mask over the DEM surface that represented the location of ice (shown in red) and a surface that should undergo modelling (shown in blue) – this ice mask is shown in figure 1B:

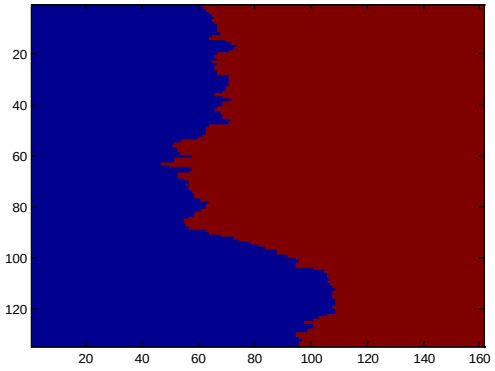


**Figure 2A: The first ice mask created to represent the ice margin at Paakitsoq (not including the Jakobshavn Isbrae glacier as the present study does not concern glaciers). The mask was created in Matlab R2006b software and the mask output illustrated is expressed in terms of 500mx500m DEM cells (134 rows and 161 columns of data).**

This ice mask was modified further (as above) to only include a limited DEM area of the study extent – the north eastern most portion of Paakitsoq, as shown by the Matlab output in figure 2B:

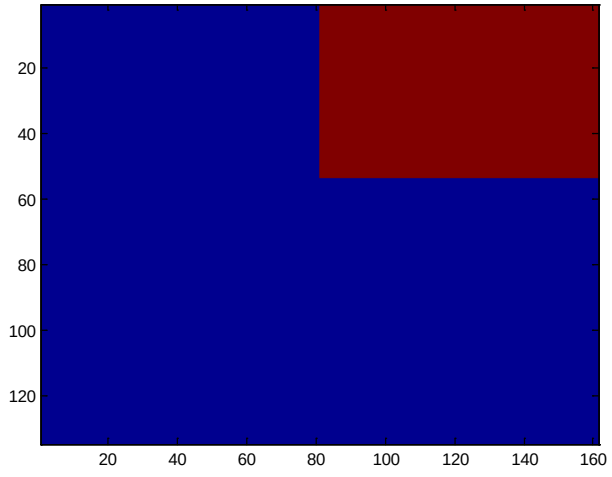


**Figure 2B: The second ice mask, representing the study area that contains numerous observed and statically modelled corresponding surface hydrological features. The extent of the modelled area is 1060km$^2$ (80 DEM cells by 53 DEM cells) compared to the initial 5393.5km$^2$ extent.**

As above, the red section of figure 2B is the extent that will be subject to modelling on running the numerical model, while the blue area will not be dealt with in the model runs. Upon a successful initial model run, this ice masked DEM extent was chosen to complete further model runs as the model was incapable of having a greater DEM extent and still functioning without error.